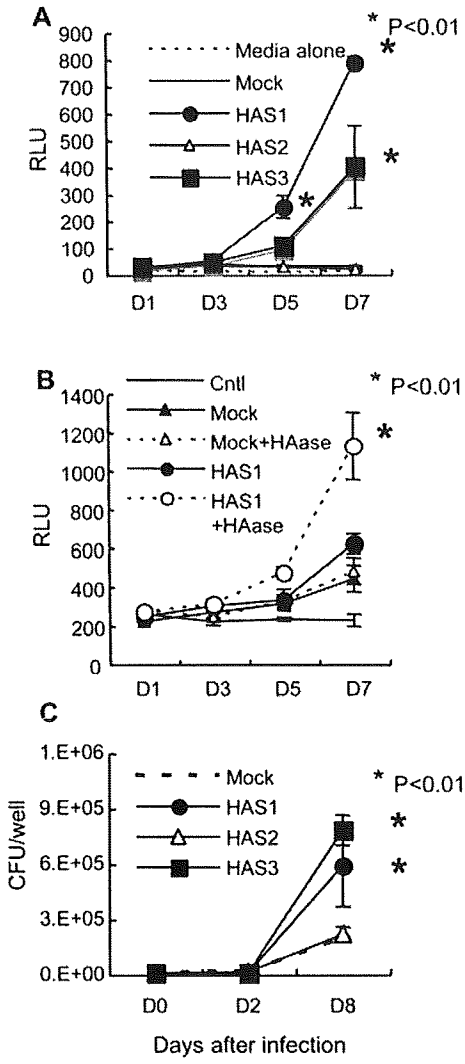

Figure 5. The effect of 3 hyaluronan synthases on the growth of BCG and *M. tuberculosis*. (A), Established transfectant cells (Rat 3Y1 fibroblasts) with control vector (Mock) or vector to express hyaluronan synthase 1 (HAS1), HAS2 (HAS2), or HAS3 (HAS3) were cultured in the presence of BCG-Luc or media alone. The growth of bacteria was monitored by luciferase activity. RLU, relative luciferase unit. The results are expressed as mean±the standard deviation ($n=3$). For statistical analysis, a two-way ANOVA with Bonferroni Post tests were used to obtain *P*-values for each time point, comparing the various growth conditions to the control. *$P<0.01$. (B), Hyaluronidase (HAase) treatment enhances the growth of BCG after infection to HAS1-tranfected cells. After 16 hours exposure of BCG-Luc to transfected cells with control vector (Mock) or vector expressing HAS1 (HAS1), unbound bacteria were washed and cultured in the presence or absence of 2 units/ml of hyaluronidase (HAase). Bacterial growth was monitored by the luciferase activity (RLU). Cntl, HAS1-transfectant cells without infection of BCG-luc. The results are expressed as mean±the standard deviation ($n=3$). For statistical analysis, a two-way ANOVA with Bonferroni Post tests were used to obtain *P*-values for each time point, comparing the various growth conditions to the control. *$P<0.01$. (C), The growth of *M. tuberculosis* H37Rv after infection to transfectant 3Y1 fibroblasts with control vector (Mock) or vector to express hyaluronan synthase 1 (HAS1), HAS2 (HAS2), or HAS3 (HAS3) was monitored by CFU. The results are expressed as mean±the standard deviation ($n=3$). For statistical analysis, a two-way ANOVA with Bonferroni Post tests were used to obtain *P*-values for each time point, comparing the various growth conditions to the control. *$P<0.01$.
doi:10.1371/journal.ppat.1000643.g005

Detection of hyaluronan in the lungs of rhesus monkeys that died of tuberculosis

M. tuberculosis-infected mice had numerous sites of granulomatous inflammation in their lungs but in primates, tuberculosis granulomas are well-organized and tighter. We next studied hyaluronan in the lung granuloma of *M. tuberculosis* H37Rv-infected rhesus monkeys by staining with alcian blue, which is commonly used dye to detect GAG. The dye stained the surrounding region of well-organized granuloma (Figure 7A) and the staining was largely abolished by treatment with hyaluronidase (Figure 7B), showing that hyaluronan is a major GAG surrounding granuloma. Acid-fast bacilli (arrow heads in Figure 7C) were located in alcian blue stained areas, thus suggesting a strong correlation between the localization of the tubercle bacilli and hyaluronan.

Vcpal suppresses mycobacterial growth *in vivo*

Finally, we addressed the effect of Vcpal on the growth of BCG in BALB/c mice. Mice were infected with BCG intravenously through their tail veins. One day after BCG challenge, the hyaluronidase inhibitor Vcpal (0.4 or 1.64 mg/dose) was injected every day thorough the tail veins for 14 days. Two days after the final injection, the mice were euthanized and viable bacteria counts were determined by the CFU assay. As a positive control, we also treated mice with amikacin (Amk), which kills extracellular but not intracellular mycobacteria, by an intramuscular injection. The results showed that Vcpal apparently suppressed growth of BCG in the lungs, similar to Amk (Figure 8).

Discussion

Although hyaluronan is crucial for both structural and physiological properties in the alveolar spaces, its role in mycobacterial infection was previously unknown. We demonstrated before that hyaluronan is the major attachment site of both BCG and *M. tuberculosis* in the infection of A549 cells, which itself produced hyaluronan [1] probably depending on HAS3 and HAS2 (Figure S2). In this study, we further extended our research and studied the role of hyaluronan after infection was established.

First, we examined the effect of hyaluronan on the growth of BCG after infection of A549 cells. BCG is an attenuated strain of the virulent *M. bovis* and is a live vaccine against tuberculosis. Because BCG bacilli share biological and pathological characteristics [33] and over 99.5% of their genome with that of *M. tuberculosis* [34], BCG is frequently utilized for the analysis of virulence of *M. tuberculosis*.

Utilizing BCG, we first found that exogenously added hyaluronan enhances the growth of BCG after incubation with A549 cells. We found that gentamicin treatment abrogated the growth of both BCG and *M. tuberculosis*, showing that these mycobacteria grow outside A549 cells. By contrast, this BCG strain (Pasteur) and *M. tuberculosis* H37Rv grew inside J774 mouse macrophages. These data apparently suggest that intracellular spaces in A549 cells are not suitable for the growth of mycobacteria.

Mycobacteria are intracellular pathogens and survive in macrophages by blocking phagosome-lysosome fusion (P-L fusion) at the stage of Rab5–Rab7 conversion [35–37]. Mycobacteria can infect non-professional epithelial cells in addition to alveolar macrophages. However, the exact mechanisms of how mycobacteria invade and persist or are killed in epithelial cells are unknown. Clemens and Horwitz demonstrated that mycobacterial phagosomes acquired Rab7 in HeLa epithelial cells, suggesting that P-L fusion is not efficiently blocked. Furthermore, Takeda's group recently found that type II pneumocytes produce antimi-

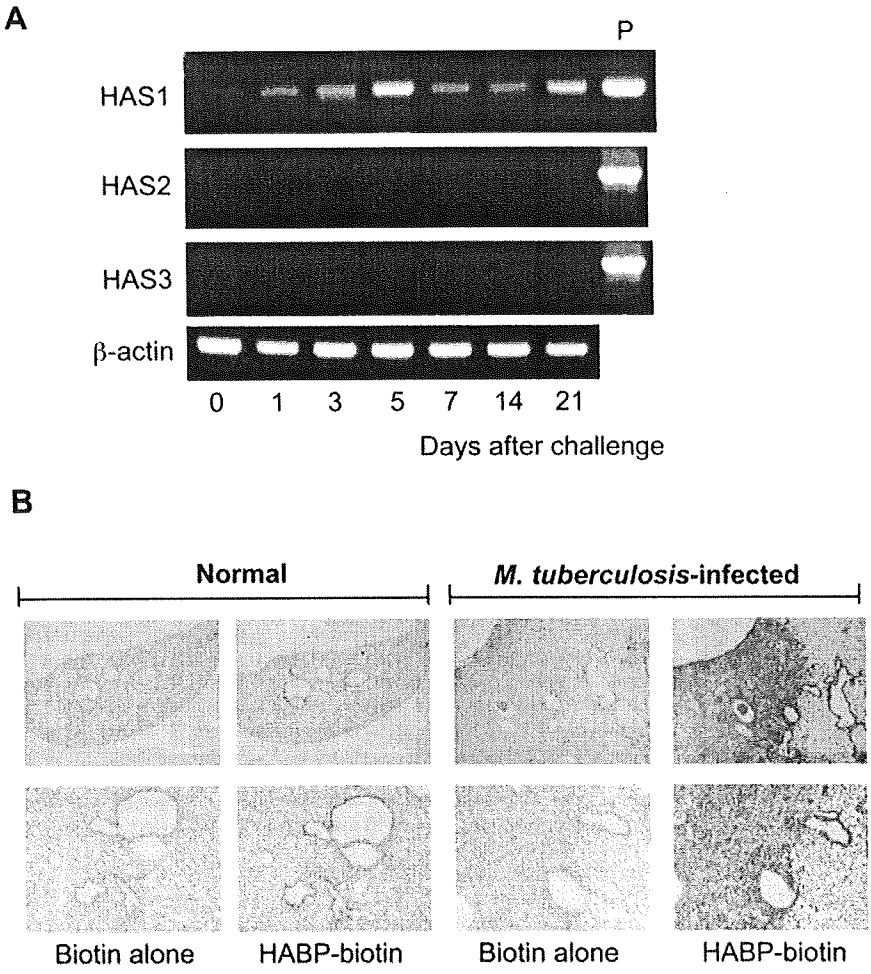

Figure 6. Production of hyaluronan during *M. tuberculosis* infection in mice. (A), BALB/c mice were aerogenically infected with *M. tuberculosis* H37Rv (around 10 CFU/lung). At the indicated periods, mice were euthanized and total RNA was extracted from the lungs. Transcription of each gene encoding HAS1, HAS2, HAS3 and beta-actin was analyzed by RT-PCR. Three mice were analyzed for each time point and representative data are presented. P, positive control of PCR employing the cDNA clone of each HAS gene as a template. (B), After euthanized, lungs from uninfected mice (Normal) or mice 21 days after infection with *M. tuberculosis* H37Rv (*M. tuberculosis* infected) were removed and histological sections were made by standard methods including formalin fixation, dehydration, and embedding in paraffin. Biotinylated hyaluronan-binding protein (HABP-biotin) was used to stain the hyaluronan in the lungs. Biotin alone was used as control straining (Biotin alone). Avidin-conjugated alkaline phosphatase and chromogen as the substrate were used to generate a red reaction product. Digital images of representative sites were acquired at ×20 (upper pictures) or ×100 (lower pictures) magnification. Experiments were performed at least three times using 5 mice for each group.
doi:10.1371/journal.ppat.1000643.g006

crobial peptides, secretory leukocyte protease inhibitor and Lipocalin 2, which have potent anti-mycobactericidal activities [5,6]. Such bactericidal molecules may contribute to the inhibition of intracellular growth of mycobacteria within type II pneumocytes. These data suggest that intracellular trafficking of mycobacteria-containing vacuoles and intracellular states of mycobacteria are different from that in macrophages.

We found that both BCG and *M. tuberculosis* grew in the media containing hyaluronan as the sole carbon source (Figure 2A and 3). In addition to hyaluronan, mammals synthesize several GAGs, but hyaluronan most strongly supported the growth of BCG among GAGs and is comparable with glucose (Figure 2). By contrast, environmental mycobacteria, such as *M. smegmatis* and *M. avium*, failed to use hyaluronan as a carbon source. These data help us to understand why pathogenic mycobacteria have the ability to adhere to hyaluronan and metabolize it. It is reasonable to assume that this property is a great advantage, allowing them to grow in the hyaluronan-rich respiratory organs of their hosts.

Because hyaluronan is a long carbon chain, we considered that cleavage must be an essential step for its use as a carbon source, and indeed found hyaluronidase activity in BCG (Figure 4). Although certain other species of bacterial pathogens, such as *Streptococcus*, *Staphylococcus*, and *Streptomyces*, produce hyaluronidases [38], there has been no report of hyaluronidase of mycobacteria. This is the first report showing hyaluronidase activity in mycobacteria.

There are two main groups of hyaluronidases identified to date. One group is endo-β-*N*-acetyl-hexosaminidase or endo-β-glucuronidase, which degrades hyaluronan by hydrolysis [39]. These enzymes are distributed in some vertebrates including mouse and human. Others are lyase type hyaluronidase that degrade hyaluronan by β-elimination [39]. Bacterial hyaluronidases are lyases, which are unstable but have stronger activity than those of vertebrates, and generate unsaturated products, which is more suitable for energy supply than saturated hyaluronan. Therefore, it is reasonable to consider that mycobacteria have the lyase type of

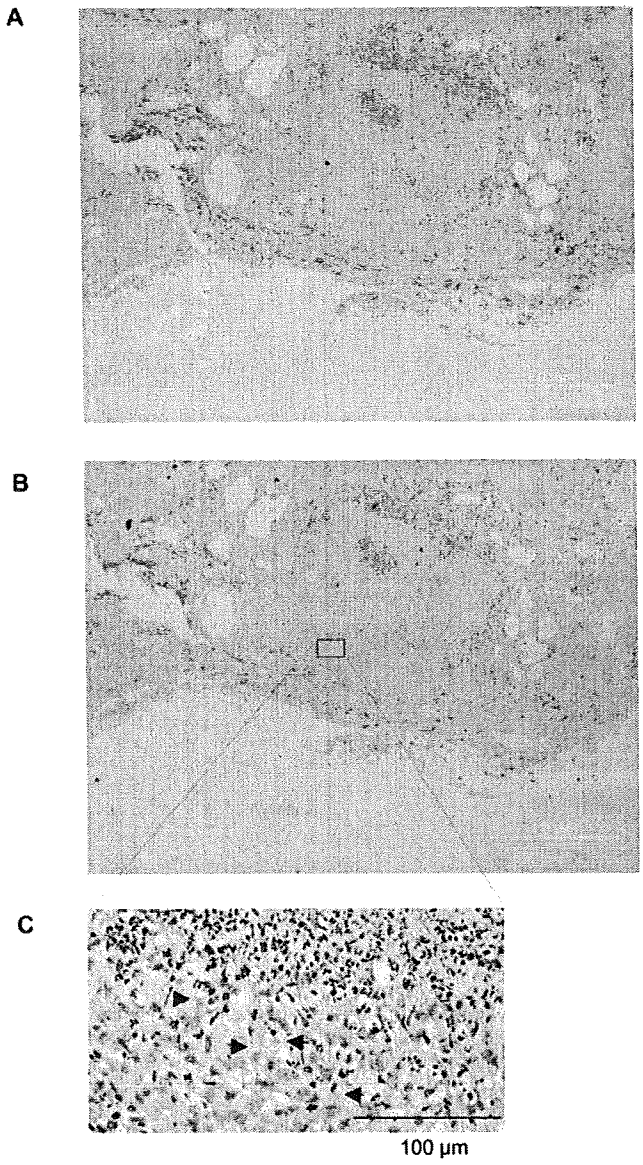

Figure 7. Presence of hyaluronan in the lungs of rhesus monkeys that died from tuberculosis. The lung sections were obtained from rhesus monkeys that had died of tuberculosis after challenge with 3,000 CFU/lung of *M. tuberculosis* H37Rv intratracheally. The sections were stained with alcian blue with (B) or without (A) pretreatment of hyaluronidase and counterstained with nuclear fast red. The section was also stained with Ziehl-Neelsen to demonstrate the presence of acid-fast bacilli (arrow heads) (C).
doi:10.1371/journal.ppat.1000643.g007

hyaluronidase. Although hyaluronidase is not yet described in the genome of either *M. tuberculosis* [33] or BCG [34], there are approximately 40 lyases. One of these lyases may be responsible for degradation of hyaluronan. Defining which enzyme is responsible for cleavage of hyaluronan is next important issue. Most hyaluronidases in mammals and bacteria display redundancy in recognition of their GAG substrates. Our data show that chondroitin sulfate also supported the growth of BCG (Figure 2). This may imply that hyaluronidase(s) of BCG cleave chondroitin sulfate as well.

Hyaluronan possesses many properties *in vivo* and it is believed that these biological activities are dependent on its size [40–42].

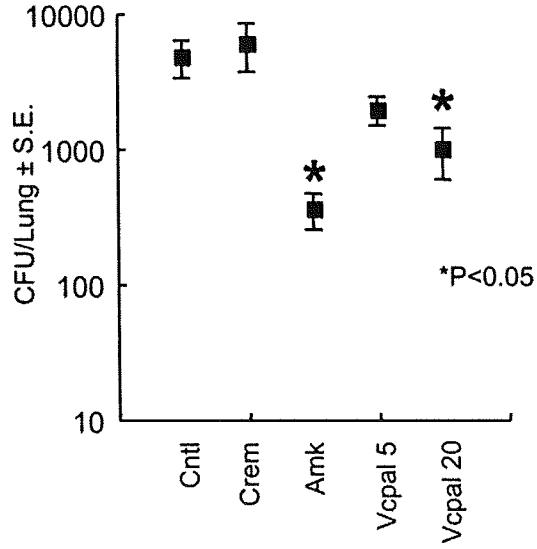

Figure 8. Vcpal suppresses the growth of mycobacteria in mouse lungs. BALB/c mice were infected with 10^6 CFU of BCG (Pasteur) intravenously. One day after the challenge, mice were treated with amikacin (Amk) and Vcpal every day for 14 days. Two days after final treatment, mice were euthanized and their lungs were homogenized. Lung pastes were serially diluted and plated in duplicate on Middlebrook 7H11 OADC agars. After incubation for 3–4 weeks at 37°C, colonies were counted and the number of CFU was calculated per lung. For statistical analysis, a two-way ANOVA with Bonferroni Post tests were used to obtain *P*-values to determine the effect of Vcpal and amikacin on bacterial growth to the control. *$P<0.05$. Cntl, control mice without treatment.
doi:10.1371/journal.ppat.1000643.g008

Although hyaluronan is composed of simple repeating disaccharides, its secondary structure is flexible. It is affected by the numbers of intramolecular hydrogen bonds, their location, and hydrophobic interactions [43,44], all of which are increased as the size of the chains increase. Dynamic laser light-scattering analysis showed that the rod-like structure of low molecular weight hyaluronan changes to a stiff coil structure beyond a molecular weight of 1×10^5 Da [45]. Taken together, it is conceivable that hyaluronan synthesized by HAS1 and HAS3 exhibits a different structure from that synthesized by HAS2. Employing HAS transfectants, we found that both BCG and *M. tuberculosis* utilize hyaluronan synthesized only by HAS1 or HAS3 for multiplication (Figure 5A and 5C).

The fact that BCG and *M. tuberculosis* grow when co-cultured with HAS1 and HAS3 but not HAS2 transfected cells (Figure 5A and 5C) suggests that HAS1 and HAS3-synthesized hyaluronan supports the growth of mycobacteria in the human body. We founds that HAS1 is the major hyaluronan synthase in *M. tuberculosis*-infected mouse lungs (Figure 6A). HAS1 is expressed in immune cells, such as dendritic cells and T cells [46]. To clarify what kind of cell expresses HAS1 during mycobacterial infection is the next important issue.

In spite of the importance of hyaluronan in host protection in the lungs, its role in mycobacterial diseases had not been elucidated. In this study, we demonstrated that BCG and *M. tuberculosis* can utilize it as a carbon source. Hyaluronan was observed in the granulomatous region of mice lungs infected with *M. tuberculosis* (Figure 6). Furthermore, *M. tuberculosis* bacilli were residing in the region where hyaluronan was located in the lungs of monkeys that had died from tuberculosis (Figure 7). We also showed that blocking hyaluronidase inhibited *in vivo* multiplication

of BCG (Figure 8). These results suggest that pathogenic mycobacteria have evolved to exploit the intrinsically host-protective molecule, hyaluronan as a nutrient to grow. Similar behavior of pathogenic mycobacteria was observed during infection of macrophages, that is, BCG is phagocytized in a cholesterol-dependent manner [47] and utilizes cholesterol as a carbon source to survive in activated macrophages [48]. It is likely that mycobacteria developed several strategies to obtain nutrients under nutrient-limited conditions.

After digestion of hyaluronan, it must be incorporated into mycobacteria through specific receptors or membrane proteins. Based on our results and consideration, hyaluronidase and a potential transporter of fragmented hyaluronan of pathogenic mycobacteria are potential drug targets.

Materials and Methods

Animal studies

All animals were maintained under specific pathogen-free conditions in the animal facilities of Osaka City University Graduate School of Medicine and in a biosafety-level-3 facility at The Research Institute of Tuberculosis according to the standard guidelines for animal experiments at each institute.

Culture medium and reagents

RPMI 1640 media, L-glutamine, fetal bovine serum, HEPES, hyaluronan from human umbilical cord, heparin from porcine intestinal mucosa and heparan sulfate from bovine kidney were purchased from Sigma-Aldrich (St. Louis, MO). Chondroitin sulfate A and C were purchased from Calbiochem (Gibbstown, NJ). For conventional culture of mycobacteria, Middlebrook 7H9 medium (Becton Dickinson) supplemented with 0.085% NaCl, 10% albumin-dextrose-catalase (BD Biosciences), 0.2% glycerol, and 0.05% Tween 80 (7H9-ADC) or 7H11-agar supplemented with 0.085% NaCl, 10% oleic acid-albumin-dextrose-catalase (BD Biosciences), and 0.2% glycerol (7H11-OADC) were used. 7H9 medium (Becton Dickinson) supplemented with 0.085% NaCl and 0.1% albumin was used as a carbon-starved 7H9 medium.

Effect of hyaluronan on extracellular growth of BCG and *M. tuberculosis* after infection to A549 cells

A549 cells were grown in RPMI 1640 medium containing 10% heat-inactivated fetal bovine serum, 2 mM L-glutamine, 25 mM HEPES and 5.5×10^{-5} M 2-mercaptoethanol (complete culture medium) at 37°C in an atmosphere of 5% CO_2. Cells were suspended at 2×10^5/ml in complete culture medium and 1 ml of cell suspension was dispensed into individual wells of a 24-well polystyrene plate (BD Biosciences, San Jose, CA). Plates were incubated at 37°C for 24 h and were washed with serum-free RPMI 1640 medium to remove nonadherent cells. Wells were then refilled with 1 ml of complete culture medium. *M. bovis* BCG or *M. tuberculosis* cell suspension was prepared as described previously [1]. The bacterial cell suspension was added to A549 cells at multiplicities of infection (MOI) of 10. After 16 (BCG) or 4 (*M. tuberculosis*) h incubation, unbound bacteria were removed by washing with serum-free RPMI 1640 three times. After adding 1 ml of fresh complete culture medium to each well, hyaluronan solution was added to final concentrations ranging from 5 to 500 μg/ml. Cells were collected periodically for luciferase or CFU assays.

Luciferase assays

Construction of BCG expressing luciferase was described previously [1]. Luciferase activity was measured using the luciferase assay system from Promega (Madison, WI) according to the manufacturer's protocol on a Wallac 1420 manager as described previously [14].

Effect of gentamicin on mycobacterial growth after infection to A549 cells

A549 cells in 96-well polystyrene plates (8×10^4/well) were infected with BCG-Luc or *M. tuberculosis* at MOI of 10 at 37°C. After 16 (BCG) or 4 (*M. tuberculosis*) h, the monolayers were washed three times with RPMI 1640 medium to remove extracellular bacteria. Fresh complete culture medium containing 1 mg/ml of hyaluronan and 50 μg/ml of gentamicin were added to each well (200 μl/well) and incubated at 37°C. Cells were collected periodically for detection of luciferase activity of BCG-Luc or CFU assay of *M. tuberculosis*.

Evaluation of glucose and GAG as carbon sources for growth of mycobacteria

BCG-Luc or *M. tuberculosis* was adjusted to a concentration of 1×10^4 CFU/ml in carbon-starved 7H9 medium described previously [14], and 200 μl of bacterial cell suspension was added to 96-well polystyrene plates. Heparin, heparan sulfate, chondroitin sulfate, hyaluronan or glucose was added to appropriate wells to a final concentration of 500 μg/ml. Plates were incubated at 37°C and bacterial cells were collected periodically for detection of luciferase activity of BCG-Luc or CFU assay of *M. tuberculosis*.

Evaluation of ingestion of hyaluronan into mycobacteria

BCG Pasteur was grown aerobically in 7H9-ADC medium at 37°C. Cells were then collected by centrifugation and half of the cells were heat-killed by heating at 65°C for 30 min. Then bacteria were washed, resuspended by carbon-starved 7H9 medium and adjusted to an optical density at 600 nm of 0.07. One hundred microliters of cell suspension was added to 100 ml of carbon-starved 7H9 with or without 6 mg of ^{3}H-labeled hyaluronan and 14 mg of non-labeled hyaluronan (final concentration of 100 mg/L of total hyaluronan). Cells were then incubated at 37°C. After incubation, cells were harvested by use of a Scatron Harvester (Scatron) onto a glass fiber filter. The incorporated radioactivity was measured in a gamma counter (ALOKA ARC-2000).

Effect of hyaluronan on mycobacterial growth

M. tuberculosis strain H37Rv, *M. smegmatis* strain mc^{2}155 and *M. avium* strain type4 were grown in carbon-starved 7H9 medium containing 0.5 mg/ml of hyaluronan, and the cultures were monitored periodically for their optical density at 600 nm (*M. tuberculosis and M. smegmatis*) or CFU (*M. tuberculosis* and *M. avium*).

Preparation of oligosaccharides from hyaluronan digested by crude extracts of BCG

BCG was grown in 7H9-ADC medium to mid-log phase. After incubation, bacterial cells were harvested, washed three times with ice-cold PBS (pH 6.0) and resuspended in the same buffer. To disrupt bacterial cells, the cell suspension was added to a screw-capped tube containing glass beads (diameter, 1.0 mm) and the tube was oscillated on a Mini-Bead Beater (Cole-Parmer). The tube was centrifuged at 10,000×*g* for 10 min, and the supernatant containing the bacterial protein extract was collected into a new tube. The protein solution was then mixed with 1 mg/ml of hyaluronan in PBS (pH 6.0) at 37°C. After incubation for 24 h, the solution was mixed with an equal volume of phenol to remove protein. The mixture was centrifuged at 10,000×*g* for 10 min and the supernatant was collected for PAGE analysis.

Polyacrylamide Gel Electrophoresis (PAGE) of hyaluronan

PAGE analysis of hyaluronan was performed as previously described by Ikegami-Kawai *et al.* [30] with minor modifications. The PAGE mini-slab gels contained 12.5% acrylamide, 0.32% *N, N'*-methylene bis-acrylamide in 0.1 M Tris-borate-1 mM Na_2EDTA (TBE, pH 8.3). For the electrophoretic run, samples containing hyaluronan were mixed with one-fifth volume of 2M sucrose in TBE and 10 µl of the mixtures was applied directly to the gel. Bromophenol blue in TBE containing 0.3 M sucrose was used as a tracking dye, but was generally applied to a well with no sample. The gels were electrophoresed at 300 V for approximately 70 min using TBE as a reservoir buffer. After electrophoresis, the gels were stained with alcian blue as described previously [30]. Briefly, the gels were soaked in 0.05% Alcian blue in distilled water for 30 min in the dark and destained in water for 30 min.

Inhibition of bacterial growth by hyaluronidase inhibitor

BCG-Luc or *M. tuberculosis* H37Rv was suspended in 7H9-ADC, carbon-starved 7H9 or carbon-starved 7H9 containing 0.5 mg/ml of hyalurona to a final concentration of 1×10^4 CFU/ml and 200µl of each suspension was added to 96-well polystyrene plates. Vcpal was added to each well. Bacterial cells were then incubated at 37°C and were collected periodically for detection of luciferase activity for BCG-Luc or CFU assay for *M. tuberculosis*. Similarly, *M. tuberculosis* H37Rv was incubated in the media containing 0.5 mg/ml hyaluronan in presence or absence of 0.1 or 0.5 mM of apigenin or quercetin. After incubation for 7 days, living bacterial number was determined by CFU assay.

RT-PCR

The expression of hyaluronan synthase genes in the lung tissues of mice aerogenically challenged with the virulent *M. tuberculosis* strain H37Rv was determined by RT-PCR. Seven-week-old of female BALB/c mice were aerogenically infected with the *M. tuberculosis* strain H37Rv (2×10^2 CFU/mouse) using a Glas-Col chamber. At different time points, 3 mice per group were euthanized and, the lungs were homogenized in PBS containing 0.05% Tween 80. The homogenates were centrifuged, and the pellets were processed to isolate total RNA using the RNeasy mini kit (QIAGEN, West Sussex, UK) according to the manufacturer's instruction. One microgram of total RNA was reverse transcribed using Super Script II RNase H reverse transcriptase (Invitrogen). The cDNA was then subjected to RT-PCR. The following primer pairs were used: β-actin, 5'-TGGAATCCTGTGGCATCCATGAAAC-3' (F) and 5'-TAAACGCAGCAGCTCAGTAACAGTCCG-3' (R); HAS1, 5'-GCTCTATGGGGCGTTCCTC-3' (F) and 5'-CACACATAAGTGGCAGGGTCC-3' (R); HAS2, 5'-TGGAACACCGGAAAATGAAGAAG-3' (F) and 5'-GGACCGAGCCGTGTATTTAGTTGC-3' (R); HAS3, 5'-CCATGAGGCGGGGTGAAGGAGAG-3' (F) and 5'-ATGCGGCCACGGTAGAAAAGTTGT-3' (R). The amplification procedure involved initial denaturation at 94°C for 4 min followed by 35 cycles of denaturation at 94°C for 1 min, annealing of primers at 57°C for 1 min and primer extension at 72°C for 3 min. After completion of the 35th cycle, the extension reaction was continued for another 7 min at 72°C.

Total RNA was extracted from A549 cells by RNeasy mini kit (QIAGEN) and then 1 µg of total RNA was reverse transcribed using Super Script II RNase H reverse transcriptase (Invitrogen). The cDNA was then subjected to RT-PCR. The following primer pairs were used: β-actin, 5'-GATCATTGCTCCTCCTGAGC-3' (F) and 5'-CACCTTCACCGTTCCAGTTT-3' (R); HAS1, 5'- ACTCGGACACAAGGTTGGAC -3' (F) and 5'- TGTACAGCCACTCACGGAAG -3' (R); HAS2, 5'- ATGCATTGTGAGAGGTTTCT -3' (F) and 5'- CCATGACAACTTTAATCCCAG -3' (R); HAS3, 5'- GACGACAGCCCTGCGTGT -3' (F) and 5'- TTGAGGTCAGGGAAGGAGAT-3' (R). The amplification procedure involved initial denaturation at 94°C for 10 min followed by 40 cycles of denaturation at 94°C for 1 min, annealing of primers at 56°C for 1 min and primer extension at 72°C for 2.5 min.

Lung sections of rhesus monkeys that died from tuberculosis

The *M. tuberculosis* H37Rv challenge infection study of in rhesus male monkeys was performed previously [49]. The lung of non-vaccinated monkeys that died of tuberculosis 3 month after intratracheal challenge of 3,000 CFU/lung of *M. tuberculosis* H37Rv were immediately removed and fixed with 15% formalin for 10 days. Three animals' lungs were embedded in paraffin blocks and used in this study as well.

Histochemical staining for hyaluronan

After deparaffinization by washing with xylene and ethanol, the tissue sections were washed in TBS and incubated with fresh TBE containing 0.05 mM of Pronase K (Dako) for 60 min at room temperature. After washing with TBS containing 1% bovine serum albumin, the slides were incubated with 3% bovine serum albumin in TBS for 30 min at room temperature to block non-specific binding sites. The slides were then washed with TBS twice for 10 min and incubated with the biotinylated hyaluronan-binding protein (HABP) probe at a concentration of 2 mg/ml in TBS for 60 min at room temperature. Following washing in TBS, the slides were incubated with a streptavidin-peroxidase reagent and the staining developed using DAKO Cytomation LSAB-system AP (Dako). The slides were then washed with distilled water and counterstained with Mayer's hematoxylin. Paraffin sections were also stained with alcian blue (Sigma) pH 2.5 (3% acetic acid) for 5 min. The slides were counterstained with nuclear fast red (Biomeda) and mounted with Gel/Mount (Biomeda). For GAG digestion, 0.5 mg/ml (10 U/ml) *Streptomyces* hyaluronidase was added for 30 min at 37°C before alcian blue staining. The slides were stained by Ziehl-Neelsen technique using carbol-fuchsin and malachite green (Sigma).

Supporting Information

Figure S1 Apigenin and quercetin suppress growth of *M. tuberculosis* in the media containing hyaluronan as a sole carbon source. *M. tuberculosis* H37Rv was cultured for 7 days in carbon-starved media (7H9) or the media containing 500 µg/ml hyaluronan as a sole carbon source (7H9-HA). Apigenin or quercetin, inhibitors of hyaluronidase, were added to be 0.5 mM or 0.1 mM. CFU was determined at time 0 (open bar) and 7 days after culture (closed bars).
Found at: doi:10.1371/journal.ppat.1000643.s001 (0.08 MB TIF)

Figure S2 Analysis of transcription of HAS genes in A549 cells. Total RNA was extracted from A549 cells cultured in RPMI1640 media containing 10% FCS. Transcription of each gene encoding human HAS1, HAS2, HAS3 and beta-actin was analyzed by RT-PCR. Three samples were analyzed and representative data are presented. M, DNA markers.
Found at: doi:10.1371/journal.ppat.1000643.s002 (0.61 MB TIF)

Acknowledgments

We are grateful to Dr. Todd P. Primm (Sam Houston State University) for editing of the manuscript and Sara Matsumoto for heartfelt encouragement.

Author Contributions

Conceived and designed the experiments: Y. Hirayama, M. Yoshimura, S. Matsumoto. Performed the experiments: Y. Hirayama, M. Yoshimura, Y. Ozeki, I. Sugawara, T. Udagawa, S. Mizuno, A. Tamaru, S. Matsumoto. Analyzed the data: Y. Hirayama, M. Yoshimura, Y. Ozeki, I. Sugawara, T. Udagawa, S. Mizuno, K. Kobayashi, S. Matsumoto. Contributed reagents/materials/analysis tools: N. Itano, K. Kimata. Wrote the paper: M. Yoshimura, I. Sugawara, H. Ogura, K. Kobayashi, S. Matsumoto.

References

1. Aoki K, Matsumoto S, Hirayama Y, Wada T, Ozeki Y, et al. (2004) Extracellular mycobacterial DNA-binding protein 1 participates in *Mycobacterium*-lung epithelial cell interaction through hyaluronic acid. J Biol Chem 279: 39798–39806.
2. Bermudez LE, Goodman J (1996) *Mycobacterium tuberculosis* invades and replicates within type II alveolar cells. Infect Immun 64: 1400–1406.
3. Hernandez-Pando R, Jeyanathan M, Mengistu G, Aguilar D, Orozco H, et al. (2000) Persistence of DNA from *Mycobacterium tuberculosis* in superficially normal lung tissue during latent infection. Lancet 356: 2133–2138.
4. Teitelbaum R, Schubert W, Gunther L, Kress Y, Macaluso F, et al. (1999) The M cell as a portal of entry to the lung for the bacterial pathogen *Mycobacterium tuberculosis*. Immunity 10: 641–650.
5. Nishimura J, Saiga H, Sato S, Okuyama M, Kayama H, et al. (2008) Potent antimycobacterial activity of mouse secretory leukocyte protease inhibitor. J Immunol 180: 4032–4039.
6. Saiga H, Nishimura J, Kuwata H, Okuyama M, Matsumoto S, et al. (2008) Lipocalin 2-dependent inhibition of mycobacterial growth in alveolar epithelium. J Immunol 181: 8521–8527.
7. Dannenberg AM, Jr. (1994) Roles of cytotoxic delayed-type hypersensitivity and macrophage-activating cell-mediated immunity in the pathogenesis of tuberculosis. Immunobiology 191: 461–473.
8. Gobin J, Horwitz MA (1996) Exochelins of *Mycobacterium tuberculosis* remove iron from human iron-binding proteins and donate iron to mycobactins in the *M. tuberculosis* cell wall. J Exp Med 183: 1527–1532.
9. Ernst JD (1998) Macrophage receptors for *Mycobacterium tuberculosis*. Infect Immun 66: 1277–1281.
10. Menozzi FD, Rouse JH, Alavi M, Laude-Sharp M, Muller J, et al. (1996) Identification of a heparin-binding hemagglutinin present in mycobacteria. J Exp Med 184: 993–1001.
11. Pethe K, Alonso S, Biet F, Delogu G, Brennan MJ, et al. (2001) The heparin-binding haemagglutinin of *M. tuberculosis* is required for extrapulmonary dissemination. Nature 412: 190–194.
12. Soares de Lima C, Zulianello L, Marques MA, Kim H, Portugal MI, et al. (2005) Mapping the laminin-binding and adhesive domain of the cell surface-associated Hlp/LBP protein from *Mycobacterium leprae*. Microbes Infect 7: 1097–1109.
13. Pethe K, Aumercier M, Fort E, Gatot C, Locht C, et al. (2000) Characterization of the heparin-binding site of the mycobacterial heparin-binding hemagglutinin adhesin. J Biol Chem 275: 14273–14280.
14. Katsube T, Matsumoto S, Takatsuka M, Okuyama M, Ozeki Y, et al. (2007) Control of cell wall assembly by a histone-like protein in mycobacteria. J Bacteriol 189: 8241–8249.
15. Itano N, Sawai T, Yoshida M, Lenas P, Yamada Y, et al. (1999) Three isoforms of mammalian hyaluronan synthases have distinct enzymatic properties. J Biol Chem 274: 25085–25092.
16. Shyjan AM, Heldin P, Butcher EC, Yoshino T, Briskin MJ (1996) Functional cloning of the cDNA for a human hyaluronan synthase. J Biol Chem 271: 23395–23399.
17. Weigel PH, DeAngelis PL (2007) Hyaluronan synthases: a decade-plus of novel glycosyltransferases. J Biol Chem 282: 36777–36781.
18. Weigel PH, Hascall VC, Tammi M (1997) Hyaluronan synthases. J Biol Chem 272: 13997–14000.
19. Camenisch TD, Spicer AP, Brehm-Gibson T, Biesterfeldt J, Augustine ML, et al. (2000) Disruption of hyaluronan synthase-2 abrogates normal cardiac morphogenesis and hyaluronan-mediated transformation of epithelium to mesenchyme. J Clin Invest 106: 349–360.
20. Aruffo A, Stamenkovic I, Melnick M, Underhill CB, Seed B (1990) CD44 is the principal cell surface receptor for hyaluronate. Cell 61: 1303–1313.
21. Yang B, Hall CL, Yang BL, Savani RC, Turley EA (1994) Identification of a novel heparin binding domain in RHAMM and evidence that it modifies HA mediated locomotion of ras-transformed cells. J Cell Biochem 56: 455–468.
22. Bartolazzi A, Peach R, Aruffo A, Stamenkovic I (1994) Interaction between CD44 and hyaluronate is directly implicated in the regulation of tumor development. J Exp Med 180: 53–66.
23. Hall CL, Yang B, Yang X, Zhang S, Turley M, et al. (1995) Overexpression of the hyaluronan receptor RHAMM is transforming and is also required for H-ras transformation. Cell 82: 19–26.
24. Jameson JM, Cauvi G, Sharp LL, Witherden DA, Havran WL (2005) Gammadelta T cell-induced hyaluronan production by epithelial cells regulates inflammation. J Exp Med 201: 1269–1279.
25. Jiang D, Liang J, Fan J, Yu S, Chen S, et al. (2005) Regulation of lung injury and repair by Toll-like receptors and hyaluronan. Nat Med 11: 1173–1179.
26. Teder P, Vandivier RW, Jiang D, Liang J, Cohn L, et al. (2002) Resolution of lung inflammation by CD44. Science 296: 155–158.
27. Termeer C, Benedix F, Sleeman J, Fieber C, Voith U, et al. (2002) Oligosaccharides of hyaluronan activate dendritic cells via toll-like receptor 4. J Exp Med 195: 99–111.
28. Forteza R, Lieb T, Aoki T, Savani RC, Conner GE, et al. (2001) Hyaluronan serves a novel role in airway mucosal host defense. FASEB J 15: 2179–2186.
29. Jacobs WR, Jr., Barletta RG, Udani R, Chan J, Kalkut G, et al. (1993) Rapid assessment of drug susceptibilities of *Mycobacterium tuberculosis* by means of luciferase reporter phages. Science 260: 819–822.
30. Ikegami-Kawai M, Takahashi T (2002) Microanalysis of hyaluronan oligosaccharides by polyacrylamide gel electrophoresis and its application to assay of hyaluronidase activity. Anal Biochem 311: 157–165.
31. Botzki A, Rigden DJ, Braun S, Nukui M, Salmen S, et al. (2004) L-Ascorbic acid 6-hexadecanoate, a potent hyaluronidase inhibitor. X-ray structure and molecular modeling of enzyme-inhibitor complexes. J Biol Chem 279: 45990–45997.
32. Li MW, Yudin AI, VandeVoort CA, Sabeur K, Primakoff P, et al. (1997) Inhibition of monkey sperm hyaluronidase activity and heterologous cumulus penetration by flavonoids. Biol Reprod 56: 1383–1389.
33. Cole ST, Brosch R, Parkhill J, Garnier T, Churcher C, et al. (1998) Deciphering the biology of *Mycobacterium tuberculosis* from the complete genome sequence. Nature 393: 537–544.
34. Brosch R, Gordon SV, Garnier T, Eiglmeier K, Frigui W, et al. (2007) Genome plasticity of BCG and impact on vaccine efficacy. Proc Natl Acad Sci U S A 104: 5596–5601.
35. Rink J, Ghigo E, Kalaidzidis Y, Zerial M (2005) Rab conversion as a mechanism of progression from early to late endosomes. Cell 122: 735–749.
36. Deretic V, Singh S, Master S, Harris J, Roberts E, et al. (2006) *Mycobacterium tuberculosis* inhibition of phagolysosome biogenesis and autophagy as a host defence mechanism. Cell Microbiol 8: 719–727.
37. Via LE, Deretic D, Ulmer RJ, Hibler NS, Huber LA, et al. (1997) Arrest of mycobacterial phagosome maturation is caused by a block in vesicle fusion between stages controlled by rab5 and rab7. J Biol Chem 272: 13326–13331.
38. Girish KS, Kemparaju K (2007) The magic glue hyaluronan and its eraser hyaluronidase: a biological overview. Life Sci 80: 1921–1943.
39. Stern R, Jedrzejas MJ (2006) Hyaluronidases: their genomics, structures, and mechanisms of action. Chem Rev 106: 818–839.
40. Hascall VC, Majors AK, De La Motte CA, Evanko SP, Wang A, et al. (2004) Intracellular hyaluronan: a new frontier for inflammation? Biochim Biophys Acta 1673: 3–12.
41. Jiang D, Liang J, Noble PW (2007) Hyaluronan in tissue injury and repair. Annu Rev Cell Dev Biol 23: 435–461.
42. Stern R, Kogan G, Jedrzejas MJ, Soltes L (2007) The many ways to cleave hyaluronan. Biotechnol Adv 25: 537–557.
43. Gribbon P, Heng BC, Hardingham TE (2000) The analysis of intermolecular interactions in concentrated hyaluronan solutions suggest no evidence for chain-chain association. Biochem J 350 Pt 1: 329–335.
44. Scott JE, Heatley F (1999) Hyaluronan forms specific stable tertiary structures in aqueous solution: a 13C NMR study. Proc Natl Acad Sci USA 96: 4850–4855.
45. Almond A, Brass A, Sheehan JK (1998) Deducing polymeric structure from aqueous molecular dynamics simulations of oligosaccharides: predictions from simulations of hyaluronan tetrasaccharides compared with hydrodynamic and X-ray fibre diffraction data. J Mol Biol 284: 1425–1437.
46. Mummert ME, Mummert D, Edelbaum D, Hui F, Matsue H, et al. (2002) Synthesis and surface expression of hyaluronan by dendritic cells and its potential role in antigen presentation. J Immunol 169: 4322–4331.
47. Gatfield J, Pieters J (2000) Essential role for cholesterol in entry of mycobacteria into macrophages. Science 288: 1647–1650.
48. Pandey AK, Sassetti CM (2008) Mycobacterial persistence requires the utilization of host cholesterol. Proc Natl Acad Sci U S A 105: 4376–4380.
49. Sugawara I, Sun L, Mizuno S, Taniyama T (2009) Protective efficacy of recombinant BCG Tokyo (Ag85A) in rhesus monkeys (Macaca mulatta) infected intratracheally with H37Rv *Mycobacterium tuberculosis*. Tuberculosis 89: 62–67.

Microbial Pathogenesis 46 (2009) 6–12

Contents lists available at ScienceDirect

Microbial Pathogenesis

journal homepage: www.elsevier.com/locate/micpath

Virulence of *Mycobacterium avium* complex strains isolated from immunocompetent patients

Yoshitaka Tateishi [a,b,*], Yukio Hirayama [a], Yuriko Ozeki [a,c], Yukiko Nishiuchi [a,d], Mamiko Yoshimura [a], Jing Kang [a], Atsushi Shibata [a], Kazuto Hirata [e], Seigo Kitada [b], Ryoji Maekura [b], Hisashi Ogura [f], Kazuo Kobayashi [g], Sohkichi Matsumoto [a,*]

[a] Department of Bacteriology, Osaka City University Graduate School of Medicine, 1-4-3 Asahi-machi, Abeno-ku, Osaka 545-8585, Japan
[b] Department of Internal Medicine, National Hospital Organization Toneyama National Hospital, 5-1-1 Toneyama, Toyonaka, Osaka 560-8552, Japan
[c] Sonoda Women's University, 7-29-1 Minamitsukaguchi-cho, Amagasaki, Hyogo 661-8520, Japan
[d] Toneyama Institute for Tuberculosis Research, Osaka City University Medical School, Toyonaka 5-1-1, Toneyama, Toyonaka, Osaka 560-8552, Japan
[e] Department of Respiratory Medicine, Osaka City University Graduate School of Medicine, 1-4-3 Asahi-machi, Abeno-ku, Osaka 545-8585, Japan
[f] Department of Virology, Osaka City University Graduate School of Medicine, 1-4-3 Asahi-machi, Abeno-ku, Osaka 545-8585, Japan
[g] Department of Immunology, National Institute of Infectious Diseases, 1-23-1, Toyama, Shinjuku-ku, Tokyo 162-8640, Japan

ARTICLE INFO

Article history:
Received 6 August 2008
Received in revised form
29 September 2008
Accepted 2 October 2008
Available online 1 November 2008

Keywords:
Mycobacterium avium complex
Virulence
Clinical isolates
Immunocompetent humans
Pulmonary disease

ABSTRACT

Mycobacterium avium complex (MAC) disease has been increasing worldwide not only in immunocompromised but also in immunocompetent humans. However, the relationship between mycobacterial strain virulence and disease progression in immunocompetent humans is unclear. In this study, we isolated 6 strains from patients with pulmonary MAC disease. To explore the virulence, we examined the growth in human THP-1 macrophages and pathogenicity in C57BL/6 mice. We found that one strain, designated 198, which was isolated from a patient showing the most progressive disease, persisted in THP-1 cells. In addition, strain 198 grew to a high bacterial load with strong inflammation in mouse lungs and spleens 16 weeks after infection. To our knowledge, strain 198 is the first isolated MAC strain that exhibits hypervirulence consistently for the human patient, human macrophages *in vitro*, and even for immunocompetent mice. Other strains showed limited survival and weak virulence both in macrophages and in mice, uncorrelated to disease progression in human patients. We demonstrated that there is a hypervirulent clinical MAC strain whose experimental virulence corresponds to the serious disease progression in the patients. The existence of such strain suggests the involvement of bacterial virulence in the pathogenesis of pulmonary MAC disease in immunocompetent status.

1. Introduction

Mycobacterium avium complex (MAC) is the most common cause of human infection due to nontuberculous mycobacteria. Initially MAC was regarded as only an opportunistic pathogen, primarily in acquired immunodeficiency syndrome (AIDS) patients [1]; however, it has now been shown to cause progressive pulmonary disease even in immunocompetent humans [2]. The American Thoracic Society indicates a wide range of clinical manifestation in patients with non-AIDS MAC disease; some patients keep a stable condition for years, whereas others progress their illness rapidly [3]. Furthermore, MAC infection can be more difficult to treat than *M. tuberculosis* due to even fewer available anti-microbial agents [3].

The pathogenesis of MAC infection has been recently investigated with respect to the host immune response. Interferon-gamma (IFN-γ) activates macrophages to produce proteolytic enzymes and other metabolites, which exhibit mycobactericidal effects. Tumor necrosis factor-alpha (TNF-α), of which production is also stimulated by IFN-γ, augments the bactericidal capacity of macrophages and plays a key role in the induction of the acquired immune response against mycobacteria [4]. A defective IFN-γ response has been shown recently to cause disseminated MAC disease in IFN-γ knock out mice and in humans with genetic mutations of IFN-γ receptor [5,6] or autoantibodies to IFN-γ in some young non-AIDS patients [7,8]. In addition to that, the activity of interleukin-10 (IL-10), which is known to inhibit cytokine synthesis by IFN-γ-producing type1 helper T cells (Th1 cells), has been shown to increase susceptibility to MAC infection in immunocompetent mice [9].

* Corresponding authors. Department of Bacteriology, Osaka City University, Graduate School of Medicine, 1-4-3 Asahi-machi, Abeno-ku, Osaka 545-8585, Japan. Tel.: +81 6 6645 3746; fax: +81 6 6645 3747.
E-mail address: y-tateishi@med.osaka-cu.ac.jp (Y. Tateishi).

0882-4010/$ – see front matter © 2008 Elsevier Ltd. All rights reserved.
doi:10.1016/j.micpath.2008.10.007

Besides genetic factors of the host, bacterial virulence should play an important role for the development of MAC disease. While isolates of *M. tuberculosis* are genetically homogeneous at the nucleotide level [10], MAC has high genetic diversity, including the presence of multiple plasmids [11], and thus likely to have a large corresponding diversity in virulence. In the most complete study examining virulence, forty-one MAC isolates from the environment as well as infected humans and animals were compared for virulence in C57BL/6 mice by intravenous injection [12]. Monitoring of the virulence by CFU counts in lungs, livers, and spleens over 4 months revealed three virulence phenotypes; high (logarithmically increasing load), intermediate (chronic infection at a constant load), and low (initial load increase followed by a decrease until clearance). In addition, clinical studies have suggested severe disease outcome in patients infected with some specific strain type of MAC. For example, MAC serovars 1, 4, and 8 *Mycobacterium avium* are associated with disease severity in AIDS patients [13], and a serovar 4 *M. avium* isolate from an AIDS patient was more invasive and proliferative in blood mononuclear cell-derived human macrophages than a serovar 2 strain from chickens [14]. In non-AIDS MAC disease, *Mycobacterium intracellulare* is associated with greater disease progression [15], and moreover, our previous prospective study on 68 non-AIDS patients suggests that serovar 4 *M. avium* is linked to greater disease progression with a pulmonary MAC infection [16]. Taking these previous data into consideration, we hypothesize that relatively hypervirulent MAC strains exist and may be associated with serious disease progression in immunocompetent patients. In order to elucidate the involvement of mycobacterial virulence in the pathogenesis of human pulmonary MAC disease, in this study we examined the difference of mycobacterial virulence of clinical isolates from patients with different disease types using human macrophages and immunocompetent mice.

2. Results

2.1. Characteristics of mycobacterial strains

Six clinical isolates of MAC were isolated from sputum of non-AIDS patients with pulmonary MAC disease, and designated 27, 33, 36, 198, 288, and 347 (Table 1). Strains 33, 198 and 288 were derived from patients with progressive disease against combination chemotherapy recommended by the American Thoracic Society guideline (progressive type) [3]. The patients with progressive disease exhibited higher levels of erythrocyte sedimentation rate (ESR), diffuse and severe pulmonary lesions in chest X-ray findings, and numerous bacteria in the sputum. The patient infected with strain 198 exhibited the most serious disease outcome among study patients in that a right pneumonectomy was needed to prevent disease progression. Strains 27, 36, and 347 were derived from patients with little progression of disease without chemotherapy (silent type). They exhibited lower levels of ESR, segmental pulmonary lesions in chest X-ray findings, and fewer bacteria in the sputum. The isolates belonging to the progressive type consisted of *M. intracellulare* unclassified serovar similar to serovar 12 (strain 198) and *M. avium* apolar type (strains 33 and 288). The isolates belonging to the silent type consisted of *M. intracellulare* serovar 1 (strain 27) and *M. avium* apolar type (strains 36 and 347). For comparison, we employed 2 veterinary strains of *M. avium* ATCC 25291 (serovar 2) as a highly virulent strain in mice [12] and ATCC 35767 (serovar 4) as a low virulent strain. Four clinical isolates other than strains 33 and 347, and ATCC 25291 formed the transparent colony morphology. Strain 33 produced both transparent and rough colony morphologies. Strain 347 and ATCC 35767 displayed smooth opaque colony morphology.

2.2. Growth of clinical isolates in 7H9 broth

All strains showed logarithmic growth from 3 days after culture in 7H9 broth (Table 2). At day 5, two isolates from progressive type (strains 198 and 288) and one isolate from silent type (strain 36) grew significantly slower than ATCC 25291 ($P < 0.005$), and all clinical strains grew significantly slower than ATCC 35767 ($P < 0.0001$). The growth of strain 198 at day 5 was significantly slower than that of strain 27 ($P = 0.001$), and was not significantly different from that of other clinical isolates.

2.3. Virulence of clinical isolates in THP-1 monocyte-derived macrophages

We next studied intracellular survival of the isolates. THP-1 cells, a human monocytic cell line, were differentiated into macrophages by treatment with phorbol 12-myristate 13-acetate (PMA) and infected with MAC strains. Strain 198 grew in THP-1 cells significantly higher than any other strains during 7 days of infection ($P < 0.0001$) (Table 3). Strain 198 grew to approximately 20-fold during 2 days of infection ($P = 0.005$), and even at day 7, it kept the same level of bacterial load as day 0. Strain 36 also grew to approximately 2-fold during 2 days of infection ($P = 0.008$); however, it was rapidly eliminated at day 7, similar to the other strains except for strain 198. There was no significant difference in

Table 1
Characteristics of isolated strains and clinical findings.

Isolates	Species and serovar	Age	Sex	Duration of illness (years)	Erythrocyte sedimentation rate (mm/h)	Chest X-ray findings[a]	Sputum[b]	
							Smear	Culture
Progressive type								
33	*M. avium* apolar type	58	M	17	62	Advanced	2+	3+
198	*M. intracellulare* unclassified serovar[c]	62	F	3	108	Advanced	2+	2+
288	*M. avium* apolar type	56	F	12	78	Advanced	2+	2+
Silent type								
27	*M. intracellulare* serovar 1	67	F	17	50	Moderate	–	1+
36	*M. avium* apolar type	54	F	9	29	Moderate	–	1+
347	*M. avium* apolar type	79	F	14	50	Moderate	1+	1+

Data and sputum samples were collected at the enrollment of the study in 2003.

[a] Advanced chest X-ray findings were defined as bilateral cavities, giant cavities, or bilateral bronchiectasis, and moderate findings were defined as focal inflammation, small or fewer cavities, or mild bronchiectasis.

[b] Smear findings of sputum were defined as follows in high performance fields of microscopy; -: no bacteria in all fields, 1+: less than one bacteria in several fields, 2+: approximately 1–12 bacteria in one field. Culture findings were defined as follows using Ogawa egg agar; 1+: colonies less than 200, 2+: colonies more than 200 and less than 500, 3+: colonies more than 500 and less than 2000.

[c] The serovar of strain 198 was identified as a new type similar to serovar 12 determined by the liquid chromatography/mass spectrometry.

Table 2
Growth rate of MAC in 7H9 broth.

Strain	Ratio of CFUs at[a]		
	Day 1	Day 3	Day 5
33	0.91 ± 0.28	38 ± 0.86	63 ± 10
198	0.93 ± 0.17	12 ± 1.9	18 ± 4.0
288	0.85 ± 0.20	4.3 ± 1.9	16 ± 0.95
27	1.1 ± 0.25	7.3 ± 2.2	120 ± 21
36	0.83 ± 0.093	5.4 ± 0.21	11.0 ± 1.7
347	0.96 ± 0.16	2.7 ± 1.1	44 ± 19
25291	1.6 ± 0.25	4.8 ± 0.24	110 ± 16*
35767	0.97 ± 0.12	11 ± 3.0	370 ± 43**

* Significantly different ($P < 0.005$) from values for strain 198, 288, and 36 as calculated by Scheffé's test.
** Significantly different ($P < 0.0001$) from values for all clinical strains as calculated by Scheffé's test.
[a] Means ± standard deviations of the ratio of CFUs to those at day 0.

the growth rate among these strains except strain 198 during infection.

On light microscopic observation, THP-1 cell morphologies were not different between infected and uninfected cells (data not shown). We then assessed cytotoxicity by the levels of lactate dehydrogenase (LDH) released into the culture supernatants at day 7. The LDH release was detectable in strain 33 and the laboratory strains (strain 33; 5.8 ± 1.5%, ATCC 25291; 11 ± 1.0%, ATCC 35767; 12 ± 1.9%, without significant difference among these strains); however, it was not detectable in other clinical isolates.

2.4. Pathogenesis of clinical isolates in mice

Female C57BL/6 mice were infected by intratracheal instillation with each strain. Bacterial load in lungs, livers, and spleens were evaluated, and histological inflammation was visually analyzed in 5-mice per strain at defined time points during 16 weeks of infection. There was no significant difference in lung CFUs among strains tested 1 day after the inoculation.

Strain 198 showed high bacterial load, and tended to increase gradually both in lungs and spleens during 16 weeks of infection ($P = 0.08$ between day 1 and 16 weeks) (Fig. 1). Strain 198 was loaded in lungs significantly higher than strain 27 ($P = 0.04$) and 33 ($P = 0.0006$) at 8 weeks of infection, and than strain 33 ($P = 0.0009$), 288 ($P = 0.001$), 36 ($P = 0.0003$), and 347 ($P = 0.004$) at 16 weeks. Histologically, strain 198 induced strong inflammation in lungs, which was paralleled with bacterial loads (Fig. 2). ATCC 25291, known as highly a virulent strain in mice [12], showed initial reduction of bacterial load in lungs at 4 weeks of infection ($P = 0.01$ between day 1 and 4 weeks) and rapid increase in bacterial load in lungs after 4 weeks of infection. ATCC 25291 was comparatively virulent to strain 198 with respect to the high bacterial load in lungs and spleens, and severe pulmonary inflammation at 16 weeks of infection. By contrast, other clinical isolates did not increase profoundly in lung CFUs; however, these strains were never eliminated from lungs. ATCC 35767 was rapidly decreased and undetectable in lungs, spleens and livers within 16 weeks of infection. Overall, the clinical isolates other than strain 198 exhibited limited histological lesions with transient inflammatory changes in lungs 4 weeks after the inoculation, and thereafter the inflammation subsided at 16 weeks.

Table 3
Growth rate of MAC in THP-1 cells.

strain	Ratio of CFUs at[a]	
	Day 2	Day 7
33	0.29 ± 0.12	0.25 ± 0.16
198	18 ± 12*	1.30 ± 0.68*
288	0.47 ± 0.26	0.097 ± 0.055
27	0.54 ± 0.37	0.28 ± 0.11
36	2.4 ± 1.2	0.31 ± 0.11
347	1.1 ± 0.49	0.36 ± 0.23
25291	0.16 ± 0.048	0.11 ± 0.038
35767	0.059 ± 0.029	0.0070 ± 0.0048

* Significantly different ($P < 0.0001$) from values for any other strains studied as calculated by Scheffé's test.
[a] Means ± standard deviations of the ratio of CFUs to those at day 0.

3. Discussion

Virulence is defined as the quantitative ability of an agent to cause disease. The virulence of mycobacteria can be evaluated by the infection to macrophages and animals [17]. This is the first study that examined the virulence of MAC isolates from immunocompetent patients with different types of disease outcome. We found that strain 198, which derived from a patient with most serious disease, revealed high bacterial load both in THP-1 cells and in C57BL/6 mice among isolates studied. Strain-specific virulence of MAC has been implicated by some previous studies of the serovar 4 *M. avium* isolated from patients. In AIDS-related MAC disease, a serovar 4 *M. avium* isolate has shown to be one of the frequently isolated type [13], and a previous analysis of a serovar 4 isolate and ATCC strain has shown the superior virulence of serovar 4 *M. avium* in human macrophages [14]. In non-AIDS pulmonary MAC disease, our recent prospective study indicates that patients infected with serovar 4 *M. avium* has poorer prognosis than those infected with MAC of other serovars [16]; however, to our best knowledge, no study has shown the direct data of mycobacterial virulence of clinical isolates and clinical disease outcome. Strain 198 is the first MAC isolate whose experimental virulence corresponds to the serious disease outcome in humans. Thus, strain 198 has strain-specific strong virulence for immunocompetent humans and mice. We consider that strain 198 is worth further genetic investigation of virulence factors.

MAC strains hypervirulent for mice has been isolated previously by Pedrosa et al. including ATCC 25291 and MAC 101, which proliferate profoundly in mouse macrophages and in mice *in vivo* [12]. In this study, strain 198 proliferated in human macrophages, in correspondence with rapid clinical disease progression and additionally in mouse lungs. The consistency between experimental virulence in human cells and clinical disease outcome suggests that the capability of inducing such strong pathogenesis may be attributed mostly to the characteristics of the pathogen, i.e. virulence factor(s) for mammalian cells unique to strain 198. Previously Birkness et al. has shown the strong cytotoxic effect and growth of serovar 4 *M. avium* isolated from an AIDS patient in blood mononuclear cell-derived human macrophages compared with a serovar 2 strain from chickens (ATCC 35713). Therefore, we evaluated cytotoxicity of MAC strains by the microscopic morphology and by the LDH release from infected THP-1 cells; however, contrary to the expectation, strain 198 was not cytotoxic to THP-1. In addition, the release of LDH was lower in strain 33, ATCC 25291, and ATCC 35767 than in the previous experiment of *M. tuberculosis* infection to THP-1 cells (cytotoxicity in cases of *M. tuberculosis* H37Rv and H37Ra; approximately 30%) [18]. We assume that cytotoxic effect may not play a major role in displaying the virulence of MAC during infection, suggested by the similar result by Huttunen et al. showing the lack of cytotoxic effect of MAC in human 28SC macrophage and A549 lung epithelial cell lines evaluated by 3-(4,5-dimethyl-2-thiazolyl)-2,5-diphenyl-2H tetrazolium bromide (MTT) assay [19]. We speculate the virulence of strain 198 depends on the ability to survive or proliferate in macrophages rather than cytotoxic effect, which, may be causative for severe pulmonary MAC disease with rapid disease progression within a few years.

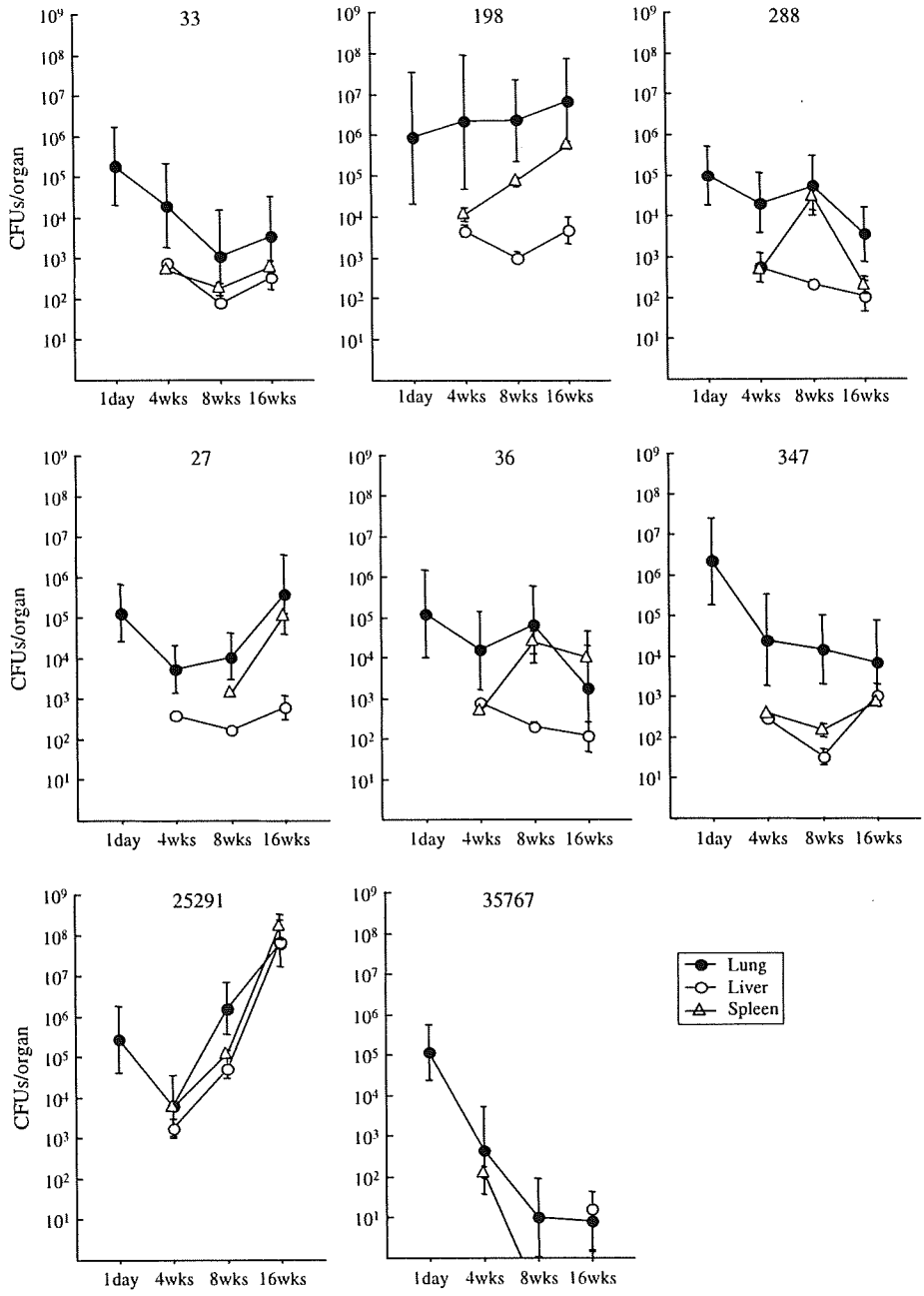

Fig. 1. Time course of mycobacterial growth in lungs, spleens and livers of C57BL/6 mice. Bacterial suspensions containing 1×10^5 CFUs were inoculated intratracheally to female C57BL/6 mice at the age of 7 weeks ($n = 20$ per strain). The lungs, livers and spleens of 5 mice per strain were sectioned at day 1 (only lungs), 4, 8, and 16 weeks later from challenge Data were presented as means ± standard deviations of CFUs/organ.

In this study, strain 198 showed strong virulence for mice at 16 weeks of infection similar to ATCC 25291; however, virulence for THP-1 cells was quite different, and pathogenic effects for mice within 4 weeks of infection was dissimilar between these two strains. These differences can be explained by the difference of immune response between host species and by the difference of immune phase. First, strain 198 could proliferate, but ATCC 25291 was rapidly eliminated in THP-1 cells (Table 3). In mouse macrophages mycobactericidal activity is attributed to nitric oxide produced by inducible nitric oxide synthase [20], whereas in human macrophages, it is attributed to Toll-like receptor signaling-dependent production of anti-microbial peptides [21,22]. Strain 198 is capable of proliferating under these two patterns of mycobactericidal activities, which suggests that strain 198 may have some virulence factors advantageous to survive both in human and mouse macrophages against mycobactericidal activity of the hosts, in contrast to ATCC 25291 which may lack virulence factors to survive in human macrophages. Second, strain 198 showed high bacterial load in lungs continuingly during 16 weeks of infection in mice, while ATCC 25291 proliferated after initial reduction in lungs at 4 weeks of infection (Fig. 1). The *in vitro* infection model using cell lines and the *in vivo* infection model using mice within 4 weeks reflects early stages of infection; on the other hand, the *in vivo* model after 8 weeks reflects chronic phase of infection [17,23]. The difference of pathogenic effects for mice within 4 weeks of infection suggests that strain 198 may resist both innate and acquired immunity, while ATCC 25291 may resist acquired immunity only. We assume that strain 198 and ATCC 25291 may possess different virulence mechanisms to persist in *in vivo* after development of acquired immunity.

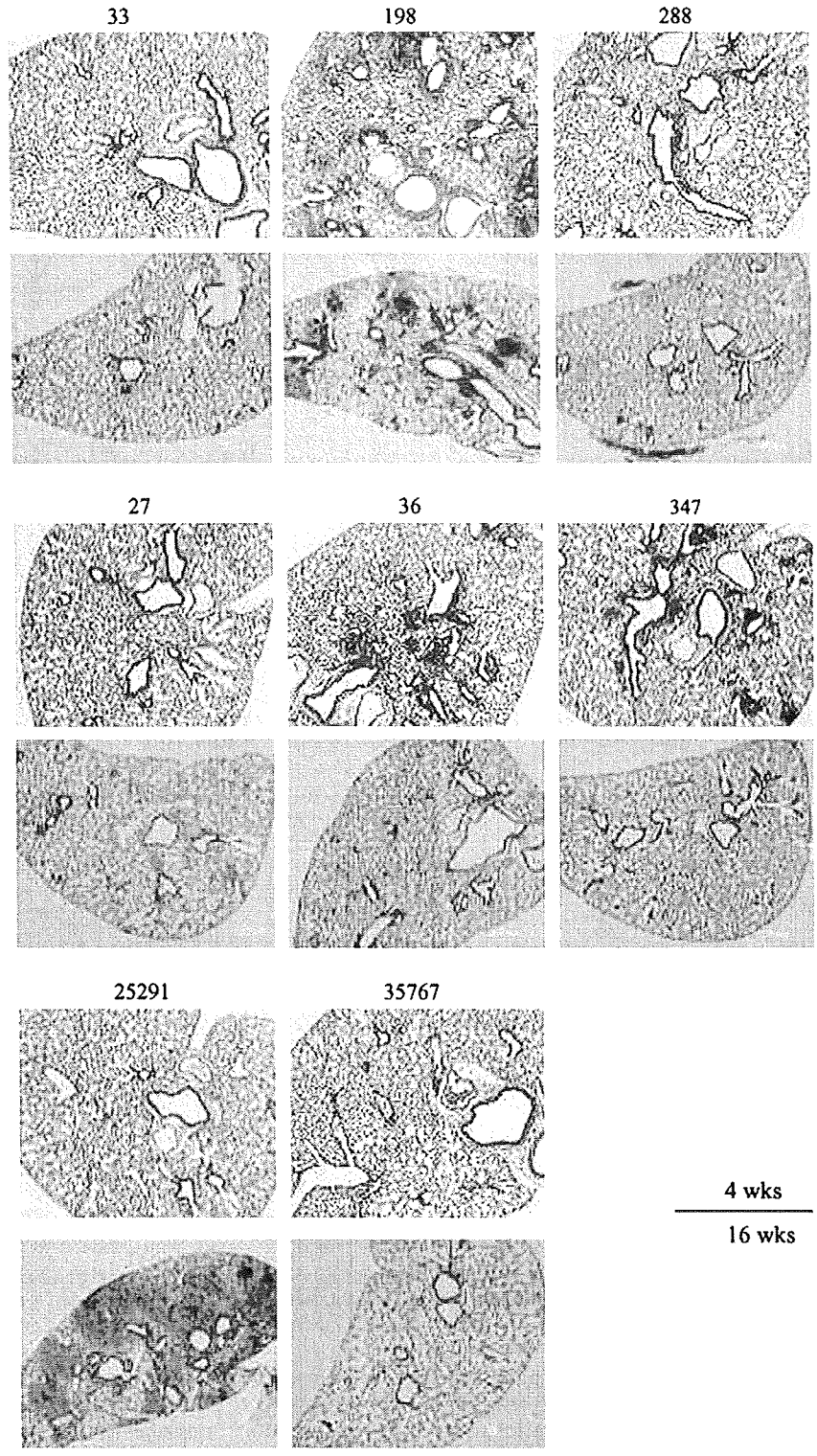

Fig. 2. Histological pictures of the lungs during 4 weeks or 16 weeks of infection in C57BL/6 mice by hematoxylin–eosin staining. Magnification, ×40.

In this study, clinical strains except for strain 198 did not show consistent virulence-associated phenotype among THP-1 cells, C57BL/6 mice, and clinical disease outcome. Similarly, Pedrosa et al. has also revealed that the growth of MAC in bone-marrow derived macrophages does not necessarily predict the virulence in mice by comparing the growth of 41 MAC isolates from various derives including humans, animals, and environment [12]. Although some clinical cases of pulmonary MAC disease may be caused by hypervirulent strains such as strain 198, these findings of clinical and natural isolates suggest that virulence may not the only determinant of the pathogenesis of pulmonary MAC disease in the majority of clinical cases. The development of pulmonary MAC disease depends on the balance between bacterial virulence and host defense. It is widely accepted that patients with pulmonary MAC disease have some characteristics of clinical background, such as males in their 40s and early 50s who have a history of cigarette smoking and excessive alcohol use, and such as postmenopausal, nonsmoking females [3], and these patient characteristics might

possibly indicate unknown predisposing conditions which enhance susceptibility for pulmonary MAC infection. The diverse phenotype of clinical MAC strains may be attributed to the disease susceptibility of the hosts. We propose that pathogenic mechanism of human pulmonary MAC disease include two patterns; one is that the strong virulence of MAC strains such as strain 198 induces rapid mycobacterial growth and serious disease outcome, and the other is that relatively weak to moderate virulence interacts with predisposing conditions of the host, leading the wide range of clinical outcome.

This study was preliminary in that we did not identify the mechanism of hypervirulence of strain 198. We observed the consistency between hypervirulence in human macrophages bedsides in immunocompetent mice and severe clinical outcome only in strain 198, not in any other isolates studied. From this finding, we speculate the existence of strain-specific virulence factors of strain 198. Recent exponential advances have enabled whole genome sequence of two *M. avium* strains, *M. avium* 104 and *M. avium* subsp. *paratuberculosis* K-10. Based on these exhaustive information, comparative genomics of MAC organisms has revealed the different genomic components regarding virulence factors, such as *ser2* encoding glycosylation enzyme of the lipopeptide core to generate the glycopeptidolipids, mammalian cell entry (*mce*) gene homologs, and PE/PPE genes (i.e., with Pro Glu and Pro Pro Glu motifs) [24]. In addition, there are large sequence polymorphisms among MAC organisms, suggesting a large corresponding diversity in virulence [11,24]. We speculate that the virulence of MAC strains including strain 198 may be determined by insertion or deletion of virulence genes encoding known [24] or unknown virulence factors.

In summary, we demonstrated that certain clinical strain derived from patients of the progressive pulmonary MAC disease exhibits strong virulence in human macrophages and in immunocompetent mice. Among clinical isolates, strain 198 is the first isolate hypervirulent to both human macrophages and mice. Our data suggest that strain-to-strain differences in virulence may play a significant role in disease progression in humans. Although Sarmento et al. showed that capability of TNF-α production from macrophages inversely correlates with the virulence of MAC strains [25], we could not find such relationship among the isolates (data not shown). In future studies, we will identify the virulence/pathogenicity-associated factor(s) of strain 198 and survey the frequency of strain variation in immunocompetent patients with pulmonary MAC disease.

4. Materials and methods

4.1. Bacterial strains

We used six clinical isolates from non-AIDS patients with pulmonary MAC disease and two laboratory strains, *M. avium* ATCC 25291 (serovar 2) and *M. avium* ATCC 35767 (serovar 4), in this study. Clinical isolates were obtained between September and November in 2003 at Toneyama National Hospital. Informed consent was obtained from all patients according to the guideline of Institutional Review Board of Toneyama National Hospital. Diagnosis of pulmonary MAC disease was made according to the American Thoracic Society guideline [3]. The samples were derived from two groups of patients; one group exhibited progressive disease in spite of the combination chemotherapy including clarithromycin, ethambutol and rifampin recommended by the American Thoracic Society guideline (progressive type) [3], the other displayed no exacerbation without anti-microbial chemotherapy for approximately ten years or more (silent type). These types were determined by the laboratory findings at the period of sputum sampling (including sputum smear and culture, chest X-ray findings, and erythrocyte sedimentation rate) and the rapidness of disease progression (Table 1). Sputum specimens were mixed with 2% sodium hydroxide, and *N*-acetyl-L-cysteine and then centrifuged for 15 min at 3000 *g*. The supernatants were discarded, and the sediment was mixed at 1:10 (vol/vol) with sterile water. The bacteria were cultivated in Middlebrook 7H9 broth supplemented with albumin–dextrose–catalase, 0.02% glycerin and 0.05% Tween 80, and then kept at −80 °C until following experiments. Identification of MAC was made by polymerase chain reaction using a commercially available kit (AMPLICOR Mycobacterium Tuberculosis Test, Roche, Basel, Switzerland). The serovars of clinical isolates were identified by the liquid chromatography/mass spectrometry as described previously [26]. Strains not containing serovar-specific oligosaccharides were defined as apolar type.

4.2. Growth in 7H9 broth

Bacterial suspension was adjusted to be 0.2 by optical density (OD) at 630 nm. The samples were cultured in 5 ml of 7H9 media in plastic tubes without agitation After vortexing to dissolve aggregates, cultivated bacterial suspensions were inoculated at days 1, 3, and 5 by serial 10-fold dilutions on Middlebrook 7H11 agar plates supplemented with oleic acid–albumin–dextrose–catalase, and 0.05% glycerol (7H11-OADC) agar plates in triplicate. The number of CFUs was counted after cultivating at 37 °C for 3 weeks.

4.3. Infection of THP-1 cells with MAC in vitro

THP-1 cells were purchased from Health Science Research Resources Bank (Tokyo, Japan). The cells were cultured in RPMI1640 containing 10% heat-inactivated fetal bovine serum (FBS; Equitech-bio, TX), and subcultured every 3–4 days. THP-1 cells were differentiated by 100 nM PMA (Sigma–Aldrich, St Louis, MO) for 48 h before infection. Before 48 h of infection, 1 ml of 2×10^5/ml cells was cultured in RPMI1640 containing 5% human serum (AB-blood group) in 24-well plates. Then, 1 ml of 2×10^4 CFUs/ml bacteria was exposed to the cultured cells for 24 h without opsonization (multiplicity of infection; 0.1 bacteria/cell). After that, the cells were treated with 20 μg/ml of gentamicin for 3 h to kill extracellular bacteria, followed by washing 4 times by RPMI1640. The infected cells were cultured in 2 ml of RPMI1640 containing 5% human serum. At days 0 and 7, uninfected bacteria were removed by washing with RPMI1640 4 times, and 500 μl of filter-sterilized phosphate buffered saline containing 0.5% Triton X-100 (Wako, Osaka, Japan) was treated per well to lyse cell membrane. The intracellular survival of bacteria was determined by counting CFUs by inoculating the cell lysate on 7H11-OADC agar plates. The experiment was performed in triplicate.

4.4. Assays for cytotoxicity

Cytotoxic effects were evaluated by the release of LDH from the cells. LDH activity of culture supernatants was determined by a commercially available kit (Roche, Basel, Switzerland). Supernatants were diluted to be 10^{-1} by distilled water for optimal reaction. The diluents were reacted with reaction mixture for 30 min, and then the OD was measured at 492 nm. Supernatants of completely lysed uninfected cells with filter-sterilized phosphate buffered saline containing 20% Triton X-100 and those of uninfected cells untreated with Triton X-100 were served as high and low controls, respectively. Cytotoxicity (%) was calculated as follows; $(OD_{sample} - OD_{low\ control}) \times 100/(OD_{high\ control} - OD_{low\ control})$. The measurement was performed in triplicate.

4.5. Animal studies

Female C57BL/6 mice aged at 6 weeks were purchased from CLEA Japan (Tokyo, Japan). All mice were kept under specific pathogen free conditions in animal facility of Osaka City University Graduate School of Medicine according to the institutional guidelines for the animal experiments. Twenty mice were used per group for infecting with each strain. One hundred microlitre of bacterial suspension containing 1×10^5 CFUs of MAC was inoculated into the trachea of the 7 weeks-aged mice anesthetized with pentobarbital sodium. Lungs, spleens and livers were removed on day 1 (only lungs) and 4, 8, 16 weeks after inoculation from 5-mice per strain. The organs were homogenized in 1 ml saline, and 0.1 ml of 10-fold dilutions of the homogenates was plated on 7H11-OADC agar followed by cultivating for 3 weeks. Bacterial burden was evaluated by CFUs per organ. Histological sections were made by standard methods including formalin fixation, dehydration, embedding in paraffin, and staining with hematoxylin and eosin.

4.6. Statistical analysis

Data were analyzed using the statistical analysis software package StatView 5.0 (SAS Institute, Cary, NC). The difference of mycobacterial growth in 7H9 broth, THP-1 cells, and mice was compared by a post hoc test of Scheffé among the strains tested. The difference of mycobacterial growth at defined time points during infection in THP-1 cells as well as in mice was compared by repeated measurement ANOVA with a post hoc test of Scheffé in the individual strains. Difference was considered statistically significant at $P < 0.05$.

Acknowledgement

We thank Todd P. Primm for the critical comments on the manuscript. We also thank Chihiro Inoue and Sara Matsumoto for the assistance of the experiments and for the heartfelt encouragement. This work was supported by grants from the Ministry of Education, Culture, Sports, Science and Technology, the Ministry of Health, Labour and Welfare (Research on Emerging and Re-emerging Infectious Diseases, Health Sciences Research Grants), The Japan Health Sciences Foundation, and The United States-Japan Cooperative Medical Science Program against Tuberculosis and Leprosy.

References

[1] Horsburgh Jr CR, Gettings J, Alexander LN, Lennox JL. Disseminated *Mycobacterium avium* complex disease among patients infected with human immunodeficiency virus, 1985–2000. Clin Infect Dis 2001;33:1938–43.
[2] Field SK, Fisher D, Cowie RL. *Mycobacterium avium* complex pulmonary disease in patients without HIV infection. Chest 2004;126:566–81.
[3] Griffith DE, Aksamit T, Brown-Elliott BA, Catanzaro A, Daley C, Gordin F, et al. An official ATS/IDSA statement: diagnosis, treatment, and prevention of nontuberculous mycobacterial diseases. Am J Respir Crit Care Med 2007;175:367–416.
[4] Flynn JL, Goldstein MM, Chan J, Triebold KJ, Pfeffer K, Lowenstein CJ, et al. Tumor necrosis factor-α is required in the protective immune response against *Mycobacterium tuberculosis* in mice. Immunity 1995;2:561–72.
[5] Dorman SE, Picard C, Lammas D, Heyne K, van Dissel JT, Baretto R, et al. Clinical features of dominant and recessive interferon γ receptor 1 deficiencies. Lancet 2004;364:2113–21.
[6] Newport MJ, Huxley CM, Huston S, Hawrylowicz CM, Oostra BA, Williamson R, et al. A mutation in the interferon-γ-receptor gene and susceptibility to mycobacterial infection. N Engl J Med 1996;335:1941–9.
[7] Kampmann B, Hemingway C, Stephens A, Davidson R, Goodsall A, Anderson S, et al. Acquired predisposition to mycobacterial disease due to autoantibodies to IFN-γ. J Clin Invest 2005;115:2480–8.
[8] Patel SY, Ding L, Brown MR, Lantz L, Gay T, Cohen S, et al. Anti-IFN-γ autoantibodies in disseminated nontuberculous mycobacterial infections. J Immunol 2005;175:4769–76.
[9] Roque S, Nobrega C, Appelberg R, Correia-Neves M. IL-10 underlies distinct susceptibility of BALB/c and C57BL/6 mice to *Mycobacterium avium* infection and influences efficacy of antibiotic therapy. J Immunol 2007;178:8028–35.
[10] Ernst JD, Trevejo-Nunez G, Banaiee N. Genomics and the evolution, pathogenesis, and diagnosis of tuberculosis. J Clin Invest 2007;117:1738–45.
[11] Primm TP, Lucero CA, Falkinham 3rd JO. Health impacts of environmental mycobacteria. Clin Microbiol Rev 2004;17:98–106.
[12] Pedrosa J, Florido M, Kunze ZM, Castro AG, Portaels F, McFadden J, et al. Characterization of the virulence of *Mycobacterium avium* complex (MAC) isolates in mice. Clin Exp Immunol 1994;98:210–6.
[13] Hoffner SE, Kallenius G, Petrini B, Brennan PJ, Tsang AY. Serovars of *Mycobacterium avium* complex isolated from patients in Sweden. J Clin Microbiol 1990;28:1105–7.
[14] Birkness KA, Swords WE, Huang PH, White EH, Dezzutti CS, Lal RB, et al. Observed differences in virulence-associated phenotypes between a human clinical isolate and a veterinary isolate of *Mycobacterium avium*. Infect Immun 1999;67:4895–901.
[15] Han XY, Tarrand JJ, Infante R, Jacobson KL, Truong M. Clinical significance and epidemiologic analyses of *Mycobacterium avium* and *Mycobacterium intracellulare* among patients without AIDS. J Clin Microbiol 2005;43:4407–12.
[16] Maekura R, Okuda Y, Hirotani A, Kitada S, Hiraga T, Yoshimura K, et al. Clinical and prognostic importance of serotyping *Mycobacterium avium–Mycobacterium intracellulare* complex isolates in human immunodeficiency virus-negative patients. J Clin Microbiol 2005;43:3150–8.
[17] Smith I. *Mycobacterium tuberculosis* pathogenesis and molecular determinants of virulence. Clin Microbiol Rev 2003;16:463–96.
[18] Danelishvili L, McGarvey J, Li YJ, Bermudez LE. *Mycobacterium tuberculosis* infection causes different levels of apoptosis and necrosis in human macrophages and alveolar epithelial cells. Cell Microbiol 2003;5:649–60.
[19] Huttunen K, Jussila J, Hirvonen MR, Iivanainen E, Katila ML. Comparison of mycobacteria-induced cytotoxicity and inflammatory responses in human and mouse cell lines. Inhal Toxicol 2001;13:977–91.
[20] Chan J, Xing Y, Magliozzo RS, Bloom BR. Killing of virulent *Mycobacterium tuberculosis* by reactive nitrogen intermediates produced by activated murine macrophages. J Exp Med 1992;175:1111–22.
[21] Liu PT, Stenger S, Li H, Wenzel L, Tan BH, Krutzik SR, et al. Toll-like receptor triggering of a vitamin D-mediated human antimicrobial response. Science 2006;311:1770–3.
[22] Thoma-Uszynski S, Stenger S, Takeuchi O, Ochoa MT, Engele M, Sieling PA, et al. Induction of direct antimicrobial activity through mammalian toll-like receptors. Science 2001;291:1544–7.
[23] Abebe F, Mustafa T, Nerland AH, Bjune GA. Cytokine profile during latent and slowly progressive primary tuberculosis: a possible role for interleukin-15 in mediating clinical disease. Clin Exp Immunol 2006;143:180–92.
[24] Turenne CY, Wallace Jr R, Behr MA. *Mycobacterium avium* in the postgenomic era. Clin Microbiol Rev 2007;20:205–29.
[25] Sarmento AM, Appelberg R. Relationship between virulence of *Mycobacterium avium* strains and induction of tumor necrosis factor α production in infected mice and in *in vitro*-cultured mouse macrophages. Infect Immun 1995;63:3759–64.
[26] Nishiuchi Y, Kitada S, Maekura R. Liquid chromatography/mass spectrometry analysis of small-scale glycopeptidolipid preparations to identify serovars of *Mycobacterium avium–intracellulare* complex. J Appl Microbiol 2004;97:738–48.

Tuberculosis 89 (2009) 252–255

Contents lists available at ScienceDirect

Tuberculosis

journal homepage: http://intl.elsevierhealth.com/journals/tube

NON-TUBERCULOUS MYCOBACTERIA: GENERAL

High transmissibility of the modern Beijing *Mycobacterium tuberculosis* in homeless patients of Japan

Takayuki Wada [a,*], Sami Fujihara [a], Akira Shimouchi [b], Makoto Harada [c], Hisashi Ogura [d], Sohkichi Matsumoto [c], Atsushi Hase [a]

[a] *Department of Microbiology, Osaka City Institute of Public Health and Environmental Sciences, 8-34 Tojo-cho, Tennoji-ku, Osaka 543-0026, Japan*
[b] *Department of Infectious Disease, Health Center of Osaka City, 1-2-7-1000 Asahi-machi, Abeno-ku, Osaka 545-0051, Japan*
[c] *Department of Bacteriology, Osaka City University Graduate School of Medicine, 1-4-3 Asahi-machi, Abeno-ku, Osaka 545-8585, Japan*
[d] *Department of Virology, Osaka City University Graduate School of Medicine, 1-4-3 Asahi-machi, Abeno-ku, Osaka 545-8585, Japan*

ARTICLE INFO

Article history:
Received 29 March 2009
Received in revised form
24 May 2009
Accepted 24 May 2009

Keywords:
Mycobacterium tuberculosis
Beijing family
VNTR
Japan
Homeless

SUMMARY

A population-based study of *Mycobacterium tuberculosis* isolated from homeless tuberculosis patients was performed during 2002–2004 in Osaka City, Japan. The data show that the ancient Beijing subfamily was predominant, whereas clustered isolates based on refined variable number of tandem repeats genotyping (19 loci) mainly belonged to the modern Beijing subfamily, suggesting its increased transmissibility.

In Japan, situated in the far eastern end of Eurasia, strains of *Mycobacterium tuberculosis*—an etiologic agent of tuberculosis (TB)—belonging to the Beijing family have been highly prevalent (approximately 75%), as in other eastern Asian countries.[1] It is well known that the Beijing family can be divided into the ancient (atypical) and the modern (typical) subfamilies.[2–5] It is presumed that the modern subfamily is more virulent and has a higher fitness to human hosts than the ancient subfamily.[2,3,6–8] Moreover, it has been speculated that the modern subfamily has been positively selected by BCG-induced immunity,[9,10] which could be attributable to the antigenic properties of the subfamily.[11,12] In a previous study, it was found that although the strains of the modern subfamily are disseminated worldwide, those of the ancient subfamily are mainly prevalent in Japan.[5]

The TB case rate in Japan has declined gradually from 25.8 per 100,000 to 19.8 during 2002–2007.[13] Osaka City, Japan, has had the highest TB case rate in Japan (about three times higher than the average: from 74.4 to 52.9 during 2002–2007). The prominent case rate observed among homeless people in the city has been considered to be the salient cause. The Airin area, in which reside about 30,000 homeless or day-laboring residents (both are strictly indistinguishable because of their fluidity), has consistently reported over 500 per 100,000 TB patients annually.[14] Generally, homelessness is regarded as a risk factor for TB incidence.[15–18] Hence, it is important to elucidate the population structure of *M. tuberculosis* in this area to control further diffusion of the infection.

To elucidate the population structure of *M. tuberculosis* isolated from TB patients among the homeless person group in Osaka City, we obtained 274 *M. tuberculosis* isolates from TB patients residing in the Airin area between January 2002 and December 2004. They were all isolates obtained from the homeless TB patients at three hospitals and two public health facilities. They covered 64.5% of the total culture-positive homeless patients in Osaka City over three years. The characteristics of patients and the drug susceptibility of the isolates are presented in Table 1. It is likely that the extremely high number of middle-aged male patients in our study reflects the general trend of the human population in that area (data not shown).

All 274 isolates were subjected to genotypic classification including the identification of Beijing family strains and the subdivision of the ancient and modern Beijing subfamilies by PCR, as described in previous reports.[5,19] Consequently, they were

* Corresponding author. Tel.: +81 6 6771 3148; fax: +81 6 6772 0676.
E-mail address: taka-wada@city.osaka.lg.jp (T. Wada).

1472-9792/$ – see front matter © 2009 Elsevier Ltd. All rights reserved.
doi:10.1016/j.tube.2009.05.007

Table 1
Characteristics of 274 homeless tuberculosis (TB) patients analyzed in this study.

Characteristics	Total (%)	Year		
		2002	2003	2004
Total	274 (100.0)	71 (100.0)	97 (100.0)	106 (100.0)
New cases	223 (81.4)	55 (77.5)	86 (88.7)	82 (77.4)
Median age [range]	57.2 [29–85]	56.9 [34–76]	57.5 [29–83]	56.8 [35–85]
Age group, y				
<35	2 (0.7)	1 (1.4)	1 (1.0)	0 (0.0)
35–44	22 (8.0)	5 (7.0)	4 (4.1)	13 (12.3)
45–54	83 (30.3)	23 (32.4)	31 (32.0)	29 (27.4)
55–64	116 (42.3)	27 (38.0)	45 (46.4)	44 (41.5)
65–74	42 (15.3)	13 (18.3)	12 (12.4)	17 (16.0)
>74	9 (3.3)	2 (2.8)	4 (4.1)	3 (2.8)
Sex				
Female	2 (7.3)	0 (0.0)	1 (1.0)	1 (0.9)
Male	272 (92.7)	71 (100.0)	96 (99.0)	105 (99.1)
Disease site				
Any pulmonary	270 (98.5)	71 (100.0)	97 (100.0)	102 (96.2)
Extrapulmonary only	4 (1.5)	0 (0.0)	0 (0.0)	4 (3.8)
Respiratory acid fast bacilli smear test results*				
Positive	218 (79.6)	60 (84.5)	78 (80.4)	80 (75.5)
Negative	52 (19.0)	11 (15.5)	19 (19.6)	22 (20.8)
Drug resistance†				
Only INH	4 (1.5)	1 (1.4)	3 (3.1)	0 (0.0)
Only RFP	3 (1.1)	2 (2.8)	0 (0.0)	1 (0.9)
MDRTB	1 (0.4)	1 (1.4)	0 (0.0)	0 (0.0)

* The results of extrapulmonary TB patients were excluded.
† INH, isoniazid; RFP, rifampin.

classified into three genetic groups according to their types: non-Beijing, ancient Beijing, and modern Beijing (Table 2). Of all isolates, Beijing family isolates were 213 (77.7%). They were further classified into 137 (50.0%; 64.3% of Beijing family) ancient subfamily isolates and 76 (27.7%; 35.7% of Beijing family) modern subfamily isolates. This population structure was consistent with the predominance of the ancient subfamily in Japan reported previously.[5]

We performed clustering analysis for all 274 isolates using variable number of tandem repeats (VNTR) genotyping methods[20] to investigate the putative direct transmission of bacilli within the population. Supply et al. reported an international set of VNTR comprising 15 genomic loci of short tandem repeats for epidemiological use (15-MIRU-VNTR).[21] Although a promising genotypic tool for global comparison, it has provided insufficient discrimination in Japanese populations of *M. tuberculosis*.[18–20] The reliable discriminatory power for epidemiological observation could be conferred by the additional hypervariable VNTR loci.[22,24,25] Therefore, we added four hypervariable loci, QUB-2163a, QUB-3232, VNTR 3820, and VNTR 4120 to the global standard. The addition of these four loci provided high discriminatory power even for Beijing family strains,[22] although they have been excluded from standard sets because of their genotypic instability and technical difficulty for comparison among different laboratories.[21,23] They were analyzed carefully by using capillary electrophoresis system, SV1210 (Hitachi Electronics).[26] All allelic profiles are listed in Table S1. Clusters were defined as two or more than two isolates with 19 identical VNTR alleles. In a total of 274 isolates, we found 114 (41.6%) clustered isolates (Table 2). The clustering rate was significantly higher in the modern Beijing subfamily (61.8%) than in the non-Beijing strains (27.9%; $P < 0.0001$, χ^2 test) and the ancient subfamily (36.5%; $P = 0.0004$, χ^2 test). We calculated the clustering rates after excluding the largest cluster(s) in order to examine whether occasional outbreaks of modern Beijing strains might be responsible for the results. On excluding one of the largest clusters (composed of 10 modern Beijing isolates) from the total population, the clustering rate was significantly higher in the modern Beijing subfamily (56.1%) than in the non-Beijing strains ($P = 0.0013$,

Table 2
Classification of Beijing family/subfamilies and clustering analysis based on VNTR* genotypings of 274 *M. tuberculosis* isolates from homeless patients in Osaka City.

	Total	Non-Beijing	Beijing	
			Ancient	Modern
No. of isolates (%)	274 (100.0)	61 (22.3)	137 (50.0)	76 (27.7)
Clustering analysis (19 loci VNTR)				
No. of type patterns	195	50	106	39
No. of unique types	160	44	87	29
No. of clusters	35	6	19	10
No. of clustered isolates	114 (41.6%)	17 (27.9%)	50 (36.5%)	47 (61.8%)
Maximum no. of isolates in a cluster	10	4	5	10
Average size of clusters	3.25	2.83	2.63	4.70
Recent transmission rate (RTI_{n-1})	0.288	0.180	0.226	0.487

* Variable number of tandem repeats.

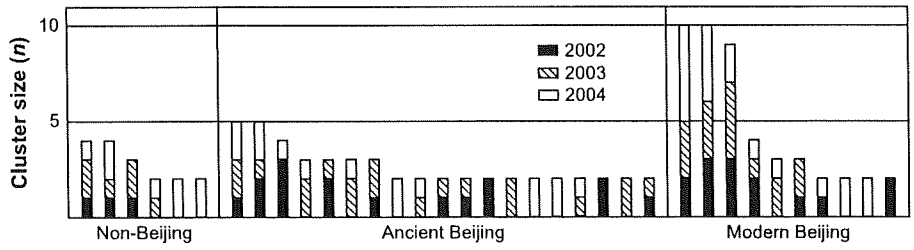

Figure 1. Distribution of all 35 clusters (114 isolates) by VNTR genotyping including 19 loci.

χ^2 test) and ancient subfamily ($P = 0.0083$, χ^2 test). On excluding the two largest clusters (20 isolates), the clustering rate in the modern Beijing family was 48.2%, which was higher than that in the non-Beijing strains ($P = 0.0232$, χ^2 test) and ancient subfamily ($P = 0.13$, χ^2 test), although the differences were not significant. When the 114 clustered isolates were analyzed by IS*6110* restriction fragment length polymorphism (RFLP) genotyping, 33 (94.3%) of 35 VNTR clusters were found to exhibit identical or less than 3 different types of band patterns (data not shown). The two exceptional clusters were found in non-Beijing strains and in the ancient Beijing subfamily; this result indicated robust cluster formation in the modern Beijing subfamily.

We introduced a recent transmission index RTI_{n-1}[27,28] (calculated by the following equation: $RTI_{n-1} = (n_c - c)/n$, where n is the total number of isolates, n_c is the number of clustered isolates, and c is the number of clusters) to quantify the transmissibility of each genotypic group. This index indicates that there is a higher likelihood of recent transmission of the modern Beijing subfamily (0.487) than of the other two groups (non-Beijing strains, 0.180; ancient Beijing subfamily, 0.226; Table 2). Previous population genetic structure analyses have revealed that the hypervariable VNTR loci exhibited high diversity (variation).[21–24] Therefore, the accordance of VNTR genotypes, including these loci, strongly supports the identification of the isolates. It is suggested that the clusters were probably formed because of active transmission in circulation, although its epidemiological links were not certified. As shown in Figure 1, the clusters by VNTR genotyping (19 loci) were classified into three groups—non-Beijing, and the ancient and modern Beijing. In our setting, we observed that large clusters were mainly observed in the modern Beijing subfamily. This result suggests that *M. tuberculosis* strains of the modern Beijing subfamily was likely to spread among homeless people to a greater extent than the other groups. Although the ancient Beijing subfamily is predominant, the population structure may be altered to resemble the worldwide typical population structure exhibiting the superiority of the modern Beijing subfamily.

Finally, we compared the clinical characterization of the homeless TB patients across the three genotypic groups (Table 3). Although higher transmissibility of the modern Beijing subfamily was speculated on the basis of the results of the clustering analysis, this subfamily did not exhibit a significant difference from other groups in the age of infected patients (vs non-Beijing, $P = 0.94$; vs ancient-Beijing, $P = 0.83$, Welch's t test) and the smear-positive rate of pulmonary TB patients (vs non-Beijing, OR = 0.51 [95% CI: 0.22–1.20]; vs ancient-Beijing, OR = 0.52 [95% CI: 0.26–1.03]). These results suggest that both the incidence of TB among younger people and the number of smear-positive cases were not associated with the higher clustering rate in the modern Beijing subfamily. This observation may lead us to understand reasons underlying the higher putative transmissibility of the modern Beijing subfamily among homeless patients. The high transmission rate of the subfamily may be associated with homelessness. It is important to analyze the population structure of

Table 3
Distribution of Characteristics of 274 homeless tuberculosis (TB) patients among Beijing family/subfamilies of causal *M. tuberculosis* isolates.

Characteristics	Total (%)	Non-Beijing (%)	Beijing	
			Ancient (%)	Modern (%)
Total	274	61	137	76
New cases	223 (81.4)	52 (85.2)	110 (80.3)	61 (80.3)
Median age [range]	57.2 [29–85]	56.8 [38–83]	57.0 [29–85]	57.4 [38–83]
Age group, y				
<35	2 (0.7)	0 (0.0)	1 (0.7)	1 (1.3)
35–44	22 (8.0)	5 (8.2)	12 (8.8)	5 (6.6)
45–54	83 (30.3)	19 (31.1)	41 (29.9)	23 (30.3)
55–64	116 (42.3)	25 (40.1)	57 (41.6)	34 (44.7)
65–74	42 (15.3)	10 (16.4)	21 (15.3)	11 (14.5)
>74	9 (3.3)	2 (3.3)	5 (3.6)	2 (2.6)
Disease site				
Any pulmonary	270 (98.5)	60 (98.3)	135 (98.5)	75 (98.7)
Extrapulmonary only	4 (1.5)	1 (1.7)	2 (1.5)	1 (1.3)
Respiratory acid fast bacilli smear test results*				
Positive	218 (79.6)	50 (83.3)	112 (81.8)	54 (71.1)
Negative	52 (19.0)	10 (16.7)	23 (16.8)	21 (27.6)
Drug resistance†				
Only INH	4 (1.5)	0 (0.0)	4 (2.9)	0 (0.0)
Only RFP	3 (1.1)	0 (0.0)	1 (0.7)	2 (2.6)
MDRTB	1 (0.4)	0 (0.0)	0 (0.0)	1 (1.3)

* The results of extrapulmonary TB patients were excluded.
† INH, isoniazid; RFP, rifampin.

TB patients other than homeless patients in order to elucidate the possibility.

In summary, the population genetic structure analysis of *M. tuberculosis* revealed that the transmission of the modern Beijing subfamily strains may be more frequent than that of other strains. The vicissitudes of population structure must be observed on the basis of up-to-date genotyping data to devise precautionary measures against the epidemic expansion of this subfamily. Our results may be linked to the dynamic observation of the process of the predominance of the modern Beijing subfamily that had occurred around Japan in the past. Further, it is also important to uncover the nature of the modern Beijing subfamily in order to ascertain the causes of its worldwide prevalence and transmission.

Acknowledgement

We are grateful to Osaka Social Medical Center, Hanna Hospital (Jinsenkai), Kawasaki Hospital, and Kanda Hospital for their support of our collection of isolates.

Funding: This work was supported by a grant from the Ministry of Health, Labour and Welfare (Research on Emerging and Re-emerging Infectious Diseases, Health Sciences Research Grants), and a grant from the US–Japan Cooperative Medical Science Program (TB Leprosy Panel).

Competing interests: None declared.

Ethical approval: Not required.

Appendix. Supplementary data

Supplementary data associated with this article can be found, in the online version, at doi:10.1016/j.tube.2009.05.007.

References

1. van Soolingen D, Qian L, de Haas PE, Douglas JT, Traore H, Portaels F, et al. Predominance of a single genotype of *Mycobacterium tuberculosis* in countries of east Asia. *J Clin Microbiol* 1995;**33**:3234–8.
2. Dou HY, Tseng FC, Lu JJ, Jou R, Tsai SF, Chang JR, et al. Associations of *Mycobacterium tuberculosis* genotypes with different ethnic and migratory populations in Taiwan. *Infect Genet Evol* 2008;**8**:323–30.
3. Mokrousov I, Ly HM, Otten T, Lan NN, Vyshnevskyi B, Hoffner S, et al. Origin and primary dispersal of the *Mycobacterium tuberculosis* Beijing genotype: clues from human phylogeography. *Genome Res* 2005;**15**:1357–64.
4. Mokrousov I, Narvskaya O, Otten T, Vyazovaya A, Limeschenko E, Steklova L, et al. Phylogenetic reconstruction within *Mycobacterium tuberculosis* Beijing genotype in northwestern Russia. *Res Microbiol* 2002;**153**:629–37.
5. Wada T, Iwamoto T, Maeda S. Genetic diversity of the *Mycobacterium tuberculosis* Beijing family in East Asia revealed through refined population structure analysis. *FEMS Microbiol Lett* 2009;**291**:35–43.
6. Bifani PJ, Mathema B, Kurepina NE, Kreiswirth BN. Global dissemination of the *Mycobacterium tuberculosis* W-Beijing family strains. *Trends Microbiol* 2002;**10**:45–52.
7. Hanekom M, van der Spuy GD, Streicher E, Ndabambi SL, McEvoy CR, Kidd M, et al. A recently evolved sublineage of the *Mycobacterium tuberculosis* Beijing strain family is associated with an increased ability to spread and cause disease. *J Clin Microbiol* 2007;**45**:1483–90.
8. Mokrousov I, Jiao WW, Sun GZ, Liu JW, Valcheva V, Li M, et al. Evolution of drug resistance in different sublineages of *Mycobacterium tuberculosis* Beijing genotype. *Antimicrob Agents Chemother* 2006;**50**:2820–3.
9. Abebe F, Bjune G. The emergence of Beijing family genotypes of *Mycobacterium tuberculosis* and low-level protection by bacille Calmette–Guérin (BCG) vaccines: is there a link? *Clin Exp Immunol* 2006;**145**:389–97.
10. Kremer K, van der Werf MJ, Au BK, Anh DD, Kam KM, van Doorn HR, et al. Vaccine-induced immunity circumvented by typical *Mycobacterium tuberculosis* Beijing strains. *Emerg Infect Dis* 2009;**15**:335–9.
11. Reed MB, Domenech P, Manca C, Su H, Barczak AK, Kreiswirth BN, et al. A glycolipid of hypervirulent tuberculosis strains that inhibits the innate immune response. *Nature* 2004;**431**:84–7.
12. López B, Aguilar D, Orozco H, Burger M, Espitia C, Ritacco V, et al. A marked difference in pathogenesis and immune response induced by different *Mycobacterium tuberculosis* genotypes. *Clin Exp Immunol* 2003;**133**:30–7.
13. The Research Institute of Tuberculosis JATA. Welcome to the Research Project for Surveillance, <http://www.jata.or.jp/rit/re/eprol_top.htm>; 2007.
14. McCurry J. Drinking too much sake in Osaka. *Lancet* 2005;**365**:375–6.
15. Barnes PF, el-Hajj H, Preston-Martin S, Cave MD, Jones BE, Otaya M, et al. Transmission of tuberculosis among the urban homeless. *Jama* 1996;**275**:305–7.
16. Nardell EA. Tuberculosis in homeless, residential care facilities, prisons, nursing homes, and other close communities. *Semin Respir Infect* 1989;**4**:206–15.
17. Potter B, Rindfleisch K, Kraus CK. Management of active tuberculosis. *Am Fam Physician* 2005;**72**:2225–32.
18. Raoult D, Foucault C, Brouqui P. Infections in the homeless. *Lancet Infect Dis* 2001;**1**:77–84.
19. Kremer K, Glynn JR, Lillebaek T, Niemann S, Kurepina NE, Kreiswirth BN, et al. Definition of the Beijing/W lineage of *Mycobacterium tuberculosis* on the basis of genetic markers. *J Clin Microbiol* 2004;**42**:4040–9.
20. Supply P, Mazars E, Lesjean S, Vincent V, Gicquel B, Locht C. Variable human minisatellite-like regions in the *Mycobacterium tuberculosis* genome. *Mol Microbiol* 2000;**36**:762–71.
21. Supply P, Allix C, Lesjean S, Cardoso-Oelemann M, Rusch-Gerdes S, Willery E, et al. Proposal for standardization of optimized mycobacterial interspersed repetitive unit-variable-number tandem repeat typing of *Mycobacterium tuberculosis*. *J Clin Microbiol* 2006;**44**:4498–510.
22. Iwamoto T, Yoshida S, Suzuki K, Tomita M, Fujiyama R, Tanaka N, et al. Hypervariable loci that enhance the discriminatory ability of newly proposed 15-loci and 24-loci variable-number tandem repeat typing method on *Mycobacterium tuberculosis* strains predominated by the Beijing family. *FEMS Microbiol Lett* 2007;**270**:67–74.
23. Murase Y, Mitarai S, Sugawara I, Kato S, Maeda S. Promising loci of variable numbers of tandem repeats for typing Beijing family *Mycobacterium tuberculosis*. *J Med Microbiol* 2008;**57**:873–80.
24. Yokoyama E, Kishida K, Uchimura M, Ichinohe S. Improved differentiation of *Mycobacterium tuberculosis* strains, including many Beijing genotype strains, using a new combination of variable number of tandem repeats loci. *Infect Genet Evol* 2007;**7**:499–508.
25. Kremer K, Au BK, Yip PC, Skuce R, Supply P, Kam KM, et al. Use of variable-number tandem-repeat typing to differentiate *Mycobacterium tuberculosis* Beijing family isolates from Hong Kong and comparison with IS *6110* restriction fragment length polymorphism typing and spoligotyping. *J Clin Microbiol* 2005;**43**:314–20.
26. Wada T, Maeda S, Hase A, Kobayashi K. Evaluation of variable numbers of tandem repeat as molecular epidemiological markers of *Mycobacterium tuberculosis* in Japan. *J Med Microbiol* 2007;**56**:1052–7.
27. Small PM, Hopewell PC, Singh SP, Paz A, Parsonnet J, Ruston DC, et al. The epidemiology of tuberculosis in San Francisco: a population-based study using conventional and molecular methods. *N Engl J Med* 1994;**330**:1703–9.
28. Durmaz R, Zozio T, Gunal S, Allix C, Fauville-Dufaux M, Rastogi N. Population-based molecular epidemiological study of tuberculosis in Malatya, Turkey. *J Clin Microbiol* 2007;**45**:4027–35.

International Journal of Systematic and Evolutionary Microbiology (2009), 59, 1336–1341 DOI 10.1099/ijs.0.000760-0

Mycobacterium kyorinense sp. nov., a novel, slow-growing species, related to *Mycobacterium celatum*, isolated from human clinical specimens

Mitsuhiro Okazaki,[1] Kiyofumi Ohkusu,[2] Hiroyuki Hata,[2] Hiroaki Ohnishi,[1] Keiko Sugahara,[3] Chizuko Kawamura,[4] Nagatoshi Fujiwara,[5] Sohkichi Matsumoto,[5] Yukiko Nishiuchi,[6] Kouichi Toyoda,[7] Hajime Saito,[8] Shota Yonetani,[1] Yoko Fukugawa,[1] Masayuki Yamamoto,[9] Hiroo Wada,[9] Akiko Sejimo,[3] Akio Ebina,[4] Hajime Goto,[9] Takayuki Ezaki[2] and Takashi Watanabe[1]

Correspondence
Hiroaki Ohnishi
onishi@ks.kyorin-u.ac.jp

[1]Department of Laboratory Medicine, Kyorin University School of Medicine, 6-20-2 Shinkawa, Mitaka-shi, Tokyo 181-8611, Japan

[2]Department of Microbiology, Regeneration and Advanced Medical Science, Gifu University Graduate School of Medicine, Gifu, 1-1 Yanagido, Gifu City, Gifu 501-1194, Japan

[3]National Hospital Organization Tokyo National Hospital, 3-1-1 Takeoka, Kiyose-shi, Tokyo 204-0023, Japan

[4]Central Laboratory, Aomori Prefectural Hospital, 2-1-1 Higashizoudou, Aomori-shi, Aomori 030-8553, Japan

[5]Department of Host Defense, Osaka City University, Graduate School of Medicine, 1-4-3 Asahi-machi, Abeno-ku, Osaka-shi 545-8585, Japan

[6]Toneyama Institute for Tuberculosis Research, Osaka City University Medical School, Osaka, Japan

[7]Kyokuto Pharmaceutical Industrial Co. Ltd, 7-8, Nihonbashi-kobunachou, Chuuou-ku, Tokyo, 103-0024, Japan

[8]Hiroshima Environment & Health Association, Health Science Center, 9-1 Hirosekita-machi, Naka-ku, Hiroshima 730-8631, Japan

[9]Department of Respiratory Medicine, Kyorin University School of Medicine, 6-20-2 Shinkawa, Mitaka-shi, Tokyo 181-8611, Japan

A novel, non-pigmented, slow-growing mycobacterium was identified on the basis of biochemical and nucleic acid analyses, as well as growth characteristics. Three isolates were cultured from clinical samples (two from sputum and one from pus in lymph nodes) obtained from three immunocompetent patients with infections. Bacterial growth occurred at 28–42 °C on Middlebrook 7H11-OADC agar. The isolates showed negative results for Tween hydrolysis, nitrate reductase, semiquantitative catalase, urease activity, 3 day arylsulfatase activity, pyrazinamidase, tellurite reduction and niacin accumulation tests, but positive results for 14 day arylsulfatase activity and heat-stable catalase tests. The isolates contained α-, keto-, and dicarboxymycolates in their cell walls. Sequence analysis revealed that all isolates had identical, unique 16S rRNA sequences. Phylogenetic analysis of the 16S rRNA, *rpoB*, *hsp65* and *sodA* gene sequences confirmed that these isolates are unique but closely related to *Mycobacterium celatum*. DNA–DNA hybridization of the isolates demonstrated less than 50 % reassociation with *M. celatum* and *Mycobacterium branderi*. On the basis of these findings, a novel species designated *Mycobacterium kyorinense* sp. nov. is proposed. The type strain is KUM 060204^T (=JCM 15038^T=DSM 45166^T).

The GenBank/EMBL/DDBJ accession numbers for the 16S rRNA, *hsp65*, *proB* and *sodA* gene sequences of strains KUM 060204^T, NTH 512-121 and AHM 060905 are, respectively: AB370111, AB370169 and AB370170 (16S rRNA); AB370171, AB370176, and AB370177 (*hsp65*); AB370178, AB370182, and AB370183 (*rpoB*); AB370184, AB370188, and AB370189 (*sodA*).

INTRODUCTION

The advent of new molecular techniques has evoked great interest in the identification and classification of non-tuberculous mycobacteria that cause infectious diseases in mammals. Currently, there are more than 100 species of non-tuberculous mycobacteria, of which approximately 60 are considered to be potential pathogens (Brown-Elliott & Wallace, 2005). Among the non-tuberculous mycobacteria, *Mycobacterium celatum* was first described by Butler *et al.* (1993). It has unique species-specific 16S rRNA and superoxide dismutase sequences, resembling those of *Mycobacterium xenopi*, but is biochemically indistinguishable from the *Mycobacterium avium* complex (Butler *et al.*, 1993). Sequencing analysis of the 16S rRNA gene in additional *M. celatum* strains revealed the existence of a new subtype, which is distinct from but very similar to the two previously reported subtypes (types 1 and 2) (Butler *et al.*, 1993). Furthermore, *Mycobacterium branderi* was described as a novel species in 1995, and analysis of its 16S rRNA sequence has confirmed the close phylogenetic relationship of this organism to *M. celatum* (Koukila-Kahkola *et al.*, 1995).

In this study, slow-growing mycobacteria with a close phylogenetic relationship to *M. celatum* were isolated from clinical specimens from three Japanese patients with infections. Biochemical tests and genotypic analyses revealed that these isolates belong to the same novel species of the genus *Mycobacterium* for which the name *Mycobacterium kyorinense* is proposed.

METHODS

Bacterial strains. Strain KUM 060204^T was isolated from the sputum of a 62-year-old Japanese man with pneumonia at Kyorin University Hospital in Mitaka City, Tokyo, Japan. Three more isolates were obtained from the sputa of the same patient at different time points, but later analyses revealed that all four isolates were identical. Therefore, these four isolates were referred to as a single strain, KUM 060204^T. Strain NTH 512-121 was isolated from the sputum of a 70-year-old Japanese man with pneumonia at the National Hospital Organization Tokyo National Hospital in Kiyose City, Tokyo, Japan. Strain AHM 060905 was isolated from pus from cervical lymph nodes of a 64-year-old Japanese woman with non-tuberculous mycobacterial lymphadenitis at Aomori Prefectural Hospital in Aomori City, Aomori, Japan. None of these three patients suffered underlying immunocompromising disease. Since strains KUM 060204^T and AHM 060905 fulfil the criteria for infections of clinical significance (Medical Section of the American Lung Association, 1997), these two strains were considered to be clinically relevant in immunocompetent patients. *M. celatum* ATCC 51131^T, *M. branderi* ATCC 51789^T and *M. branderi* ATCC 51788 were purchased from ATCC and used as standard strains.

Phenotypic properties. Bacterial morphology and acid–alcohol-fastness were determined by Ziehl-Neelsen staining as described by Chapin (2007). Colony morphology, pigmentation, and the ability of the isolates to grow at various temperatures (25, 28, 30, 35 and 42 °C) were observed on Middlebrook 7H11-OADC agar (Nippon Becton Dickinson) and 1% Ogawa egg agar (Kyokuto Pharmaceutical Industrial Co. Ltd). The following biochemical tests were performed as described by Kent & Kubica (1985): Tween hydrolysis, nitrate reductase, pyrazinamidase, tellurite reduction, urease activity, niacin accumulation, arylsulfatase activity (3- and 14-day), semiquantitative catalase and heat-stable catalase tests (68 °C).

Antimicrobial susceptibility testing. MICs for amikacin, clarithromycin, ethambutol, isoniazid, kanamycin, levofloxacin, rifampicin and streptomycin were determined based on the broth microdilution method with Broth MIC NTM (Kyokuto Pharmaceutical Industrial Co. Ltd) as described in monograph M24-A of the National Committee on Clinical Laboratory Standards, now CLSI (NCCLS, 2003).

Mycolic acid analysis by thin-layer chromatography (TLC). Mycolic acid analyses were performed using Silica gel TLC (Uniplate, 20 × 20 cm, 250 μm; Analtech) and matrix-assisted laser desorption/ionization time-of-flight mass spectrometry (MALDI-TOF MS) with an Ultraflex II (Bruker Daltonics) as described previously (Masaki *et al.*, 2006) with some modifications. *Mycobacterium tuberculosis* H37Rv ATCC 27294^T, *M. avium* ATCC 25291^T and *Mycobacterium intracellulare* ATCC 13950^T were used as controls.

Sequence determination and phylogenetic analysis. DNA was prepared after mechanical disruption of bacterial cells and subjected to sequence analysis of the 16S rRNA, *hsp65*, *rpoB* and *sodA* genes using methods as described by Kirschner *et al.* (1993), Telenti *et al.* (1993), Boor *et al.* (1995) and Domenech *et al.* (1997) with some modifications. Phylogenetic trees with bootstrap values were generated using the CLUSTAL W program (www.clustal.org) and displayed using TREEVIEW as described by Li *et al.* (2004). Phylogenetic analyses were also performed using the neighbour-joining method with Kimura's two-parameter distance correction model with 100 bootstrap replications in the MEGA version 2.1 software package. Homology searching with the 16S rRNA, *hsp65*, *rpoB* and *sodA* gene sequences was performed against sequences registered in GenBank/EMBL/DDBJ using BLAST.

DNA–DNA hybridization. Quantitative microplate DNA–DNA hybridization for selected strains was carried out under optimal conditions as described by Ezaki *et al.* (1988, 1989).

RESULTS AND DISCUSSION

The three isolates examined were acid–alcohol-fast, non-motile, non-spore-forming bacilli. Mature colonies of all isolates developed in 4 weeks on Middlebrook 7H11-OADC agar. Growth was observed at temperatures in the range 28–42 °C, with optimal growth obtained at 30–35 °C. No growth was observed at 25 °C. Colonies were smooth and initially transparent, but became creamy white on prolonged culture.

All three isolates were negative for Tween hydrolysis, nitrate reductase, semiquantitative catalase, urease activity, 3-day arylsulfatase activity, pyrazinamidase, tellurite reduction and niacin accumulation, but positive for 14-day arylsulfatase activity and heat-stable catalase (Table 1). All isolates were distinguishable from *M. celatum* and *M. branderi* by a lack of growth at 25 °C and a negative pyrazinamidase test. They were also distinguishable from *M. celatum* by a negative result for 3-day arylsulfatase activity and the tellurite reduction test. The three isolates were also distinct from *Mycobacterium cookii* by their ability to grow at 45 °C and a lack of growth at 25 °C, absence of pigment production in the dark, and a negative semiquantitative catalase test. They were also distinct from

Table 1. Growth characteristics of strain KUM 060204^T in comparison with the closely related species *M. celatum* and *M. branderi*

+, Positive; –, negative; ND, not done.

Characteristic	KUM 060204^T	*M. celatum**	*M. branderi**
Growth temperature (°C)			
25	–	+	+
28	+	+	ND
30	+	+ (31 °C)	ND
35	+	ND	ND
42	+	+ (45 °C)	+ (45 °C)
Heat-stable catalase (68 °C)	+	+	–
Arylsulfatase activity			
3 days	–	+	–
14 days	+	+	+
Pyrazinamidase	–	+	+
Tellurite reduction	–	+	ND

*Data taken from Butler *et al.* (1993), Koukila-Kahkola *et al.* (1995) and Vincent & Gutierres (2007).

M. xenopi by the lack of pigment production in the dark (Koukila-Kahkola *et al.*, 1995).

Using antimicrobial susceptibility tests, all isolates were shown to be susceptible to clarithromycin and ethambutol, but resistant to isoniazid and rifampicin. Amikacin, kanamycin, levofloxacin and streptomycin showed low MIC values against all three isolates (Table 2).

Mycolic acid analyses of the three isolates by TLC produced identical multispot patterns composed of α- (C82-86)-, keto (C84-89)- and dicarboxy- (C64-69) mycolates. The length of the carbon chain of each mycolic acid methyl ester was assigned by the mass number and proposed structures as summarized in Table 3. The mycolic acids contained predominantly one or two cyclopropane rings. This pattern of mycolic acid subclasses is characteristic for the *Mycobacterium avium* complex, and is also seen in *M. celatum* and *M. branderi*, suggesting that the new isolates are closely related to these *Mycobacterium* species (Fig. 1) (Butler *et al.*, 1993; Brander *et al.*, 1992).

Table 2. Susceptibility of the three isolates to various antibiotics

Antibiotic	MIC (μg ml^{-1})		
	KUM 060204^T	NTH 512-121	AHM 060905
Amikacin	<0.5	<0.5	<0.5
Clarithromycin	<0.03	<0.03	<0.03
Ethambutol	4	2	4
Isoniazid	16	32	16
Kanamycin	0.5	0.25	1
Levofloxacin	0.125	<0.03	0.125
Rifampicin	32	>32	>32
Streptomycin	0.25	0.25	0.25

The sequence of the 16S rRNA gene was identical in all strains, but was different from all other available 16S rRNA sequences. The sequences of the *hsp65*, *rpoB* and *sodA* genes were also identical in the three isolates. It was assumed that these three isolates belong to the same species, and strain KUM 060204^T was used as a representative strain for genotypic analyses thereafter.

Sequence analysis revealed that the 16S rRNA gene sequence of the newly identified mycobacterium was closest to that of *M. celatum* ATCC 51130 (type 2) with 18 base mismatches out of 1469 bp (98.8 % identity). It was also highly similar to that of *M. celatum* NCTC 12882 (type 3) with 25 base mismatches out of 1476 bp (98.3 %), *M. celatum* ATCC 51131^T (type 1) with 27 base mismatches out of 1450 bp (98.1 %), *M. branderi* ATCC 51789^T with 32 base mismatches out of 1476 bp (97.8 %) and *M. cookii* ATCC 49103^T with 41 base mismatches out of 1477 bp (97.2 %). A phylogenetic tree was created based on the 16S rRNA gene sequences, incorporating all previously described species of slow-growing mycobacteria. Phylogenetic analysis revealed that strain KUM 060204^T is adjacent to the type strains of *M. celatum* (ATCC 51131^T), *M. branderi* (ATCC 51789^T) and *M. cookii* (ATCC 49103^T) (Fig. 2a).

The *hsp65* gene sequence of strain KUM 060204^T was identical to that of *M. celatum* ATCC 51130 (392/392, 100 %) and highly similar to those of *M. branderi* ATCC 51789^T and *M. celatum* ATCC 51131^T (98.8 and 98.1 %, respectively). A phylogenetic tree based on the *hsp65* sequences is shown in Fig. 2(b). Phylogenetic analysis of the *hsp65* gene gave consistent results, i.e. strain KUM 060204^T is located adjacent to the type strains of *M. branderi* (ATCC 51789^T) and *M. celatum* (ATCC 51131^T).

The sequence of the *rpoB* gene of strain KUM 060204^T was identical to that of *M. celatum* ATCC 51130 (306/306, 100 %) and highly similar to that of *M. branderi* ATCC 51789^T (96.7 %). It showed further differences from those of *M. celatum* ATCC 51131^T and *M. cookii* ATCC 49103^T (94.1 and 92.7 %, respectively). Strain KUM 060204^T clustered adjacent to *M. branderi* ATCC 51789^T and *M. celatum* ATCC 51131^T (Fig. 2c) in a phylogenetic tree based on *rpoB* sequences.

The *sodA* gene of strain KUM 060204^T was almost identical to that of *M. celatum* ATCC 51130 (411/413, 99.5 %) and highly similar to that of *M. celatum* ATCC 51131^T (96.6 %). It showed further differences from those of *M. branderi* ATCC 51789^T and *M. xenopi* ATCC 19250^T (90.1 and 86.4 %, respectively) (Fig. 2d).

Given the close relationship of strain KUM 060204^T to *M. celatum* and *M. branderi*, a DNA–DNA hybridization study was performed for these strains under optimal conditions (Table 4). Strain KUM 060204^T exhibited DNA similarity values below the suggested species threshold (70 %) to its